Pure Appl. Geophys. 168 (2011), 2395–2425

DOI 10.1007/s00024-011-0354-7

Pure and Applied Geophysics

Earthquake Rupture at Focal Depth, Part I: Structure and Rupture of the Pretorius Fault, TauTona Mine, South Africa

V. Heesakkers,[1,2] S. Murphy,[1,3] and Z. Reches[1]

Abstract—We analyze the structure of the Archaean Pretorius fault in TauTona mine, South Africa, as well as the rupture-zone that recently reactivated it. The analysis is part of the Natural Earthquake Laboratory in South African Mines (NELSAM) project that utilizes the access to 3.6 km depth provided by the mining operations. The Pretorius fault is a ~10 km long, oblique-strike-slip fault with displacement of up to 200 m that crosscuts fine to very coarse grain quartzitic rocks in TauTona mine. We identify here three structural zones within the fault-zone: (1) an outer damage zone, ~100 m wide, of brittle deformation manifested by multiple, widely spaced fractures and faults with slip up to 3 m; (2) an inner damage zone, 25–30 m wide, with high density of anastomosing conjugate sets of fault segments and fractures, many of which carry cataclasite zones; and (3) a dominant segment, with a cataclasite zone up to 50 cm thick that accommodated most of the Archaean slip of the Pretorius fault, and is regarded as the 'principal slip zone' (PSZ). This fault-zone structure indicates that during its Archaean activity, the Pretorius fault entered the mature fault stage in which many slip events were localized along a single, PSZ. The mining operations continuously induce earthquakes, including the 2004, M2.2 event that rejuvenated the Pretorius fault in the NELSAM project area. Our analysis of the M2.2 rupture-zone shows that (1) slip occurred exclusively along four, pre-existing large, quasi-planer segments of the ancient fault-zone; (2) the slipping segments contain brittle cataclasite zones up to 0.5 m thick; (3) these segments are not parallel to each other; (4) gouge zones, 1-5 mm thick, composed of white 'rock-flour' formed almost exclusively along the cataclasite-host rock contacts of the slipping segments; (5) locally, new, fresh fractures branched from the slipping segments and propagated in mixed shear-tensile mode; (6) the maximum observed shear displacement is 25 mm in oblique-normal slip. The mechanical analysis of this rupture-zone is presented in Part II (Heesakkers *et al.*, Earthquake Rupture at Focal Depth, Part II: Mechanics of the 2004 M2.2 Earthquake Along the Pretorius Fault, TauTona mine, South Africa 2011, this volume).

Key words: Brittle faulting, fault reactivation, earthquake mechanics, earthquake rupture zone, deep mine, fault rocks.

1. Introduction

Fault-zones typically move by infrequent earthquakes that are localized along weak surfaces and separated by inter-seismic periods of tens to thousands of years. Fault healing between earthquakes may renew fault strength and its rupture resistance (Marone, 1998; Muhuri *et al.*, 2003; Sibson, 1985). This earthquake cycle terminates when the fault becomes quiescent due primarily to changes in tectonic activity. However, ancient faults may be reactivated after long quiescence periods (Holdsworth *et al.*, 1997), for example, fault reactivation with slip inversion along faults in the Colorado Plateau, Arizona, after >1 Ga of inactivity (Reches, 1978; Huntoon, 1974). Healing processes during such long periods of inactivity would modify and may strengthen the existing faults. Our central objective is to analyze the neo-tectonic reactivation and rupture processes of faults that were inactive for long time periods, and we selected the extreme case of the Pretorius fault, TauTona mine, South Africa, that has been inactive for at least 2 Ga and has been reactivated by recent mining operations. The mine allows for direct, in situ analysis of the fault-zone and its mechanical conditions. We follow previous studies of earthquake ruptures in deep South African mines that documented failure of intact rock in unfaulted regions (Gay and Ortlepp, 1979; Ortlepp, 1992, 2000; Ogasawara *et al.*, 2002a, b), or reactivation of ancient faults, e.g., rupturing the Dagbreek fault, Welkom, South Africa, during the M4.6, Matjhabeng earthquake, 1999 (Dor *et al.*, 2001). The study includes two parts. Part I (present) includes the structural characterization of the Pretorius fault, and description of the rupture-zone of the 2004, M2.2

[1] School of Geology and Geophysics, University of Oklahoma, Norman, OK, USA. E-mail: reches@ou.edu

[2] *Present Address*: Chevron ETC, 1500 Louisiana St, Houston, TX 77002, USA.

[3] *Present Address*: AngloGold Ashanti, Carletonville, Gauteng, South Africa.

earthquake along it. Part II (Heesakkers *et al*., 2011, this volume) presents the mechanical analysis of this seismic reactivation based on the rupture zone structures and mechanical properties of the fault rocks.

In the present part, we first outline the tectonic setting of the study area, and then describe the multi-scale, 3D structure of the fault-zone, including the image logs analysis of fractures in boreholes drilled within and near the Pretorius fault. Finally, we discuss the structural development of the Pretorius fault, the origin of its fault rocks, and the characteristics of the M2.2 rupture-zone.

2. NELSAM Project

The present study is part of the Natural Earthquake Laboratory in South African Mines (NELSAM) project, which was designed to investigate seismogenic processes at focal-depths in deep gold mines in South Africa (Reches, 2006; Reches and Ito, 2007). The mines provide a unique setting with in situ access to hypocenters of earthquakes of moment-magnitude -2 to ~ 4, with the larger magnitudes often occurring along pre-existing fault-zones. Mining operations control the location, magnitude and timing of the earthquakes (Cook, 1963; Spottiswoode and McGarr, 1975; McGarr, 1984; Gibowicz and Kijko, 1994; Mendecki, 1997; Ogasawara *et al*., 2002a, b), and allow for monitoring at distances of 1–100 m from anticipated hypocenters (Yabe *et al*., 2009). The NELSAM objectives that are addressed here include the characterization of a reactivated fault-zone, determination of the stress/strain/strength distribution in the vicinity of this fault, and analysis of the rupture dynamic processes.

The main research site is located on the Pretorius fault that is exposed at a depth of 3.6 km in TauTona mine, about 80 km west of Johannesburg, South Africa (Fig. 1). The Pretorius fault was formed ~ 2.7 Ga ago and has been inactive during the last 2.0 Ga. Currently, it is being reactivated by the active mining in TauTona mine (van Aswegen and Butler, 1993). The NELSAM laboratory site covers an area 90,000 m^2, at a depth of ~ 3.6 km, in the south side of TauTona mine (Fig. 2a) close to the southward mining development. Within this site, a total of 18 vertical and inclined boreholes were drilled within tunnels at two mining levels, levels 118 and 120, that are 11,800 and 12,000 ft below ground level, respectively. In the boreholes around the Pretorius fault, we installed 3D broadband accelerometers, seismometers, EM electrodes, and a 110 m long strain meter that crosses the Pretorius fault. In addition, gas emission monitoring system with onsite mass-spectrometer and gamma detector and a microbial monitoring system were installed at level 118 of the NELSAM laboratory site (Onstott *et al*., 2008; Lippmann-Pipke *et al*., 2009). The instruments' layout at the NELSAM site was based on the structural characterization of the Pretorius fault presented here.

3. Tectonic Setting

3.1. The Witwatersrand Basin

The Pretorius fault is located in the Western Deep Levels of the Archaean Witwatersrand Basin, South Africa (Fig. 1), which is the world's largest known gold province. The basin is a 350 × 200 km NE trending structure that developed in a foreland thrust setting during the convergence of the Zimbabwe plate and the Kaapvaal Craton, during the later stage of the West Rand, about 2.9 Ga ago (Gibson *et al*., 2000b; Robb *et al*., 1997). The basin accumulated the Witwatersrand Supergroup sediments of 2.71–2.97 Ga ago, a 7–10 km thick sequence of terrigenous sedimentary rocks, comprising mainly of sandstones and mudrock, together with minor conglomerate horizons (Armstrong *et al*., 1991; Gibson *et al*., 2000b; Robb *et al*., 1997). The region experienced continuous thrusting into the Central Rand stage until 2.7 Ga BP (Gibson *et al*., 2000b). The sedimentation was followed by up to 3 km thick tholeiitic flood basalts from the Ventersdorp Supergroup during the Platberg rifting. This was followed by up to 2 km of local rift sediments (Gibson *et al*., 2000b). Most of the Kaapvaal Craton was covered by a shallow sea 2.6 Ga ago, after which a period of slow subsidence was followed by deposition of the 2–3 km thick Pretoria Group. At the later stage of the Platberg

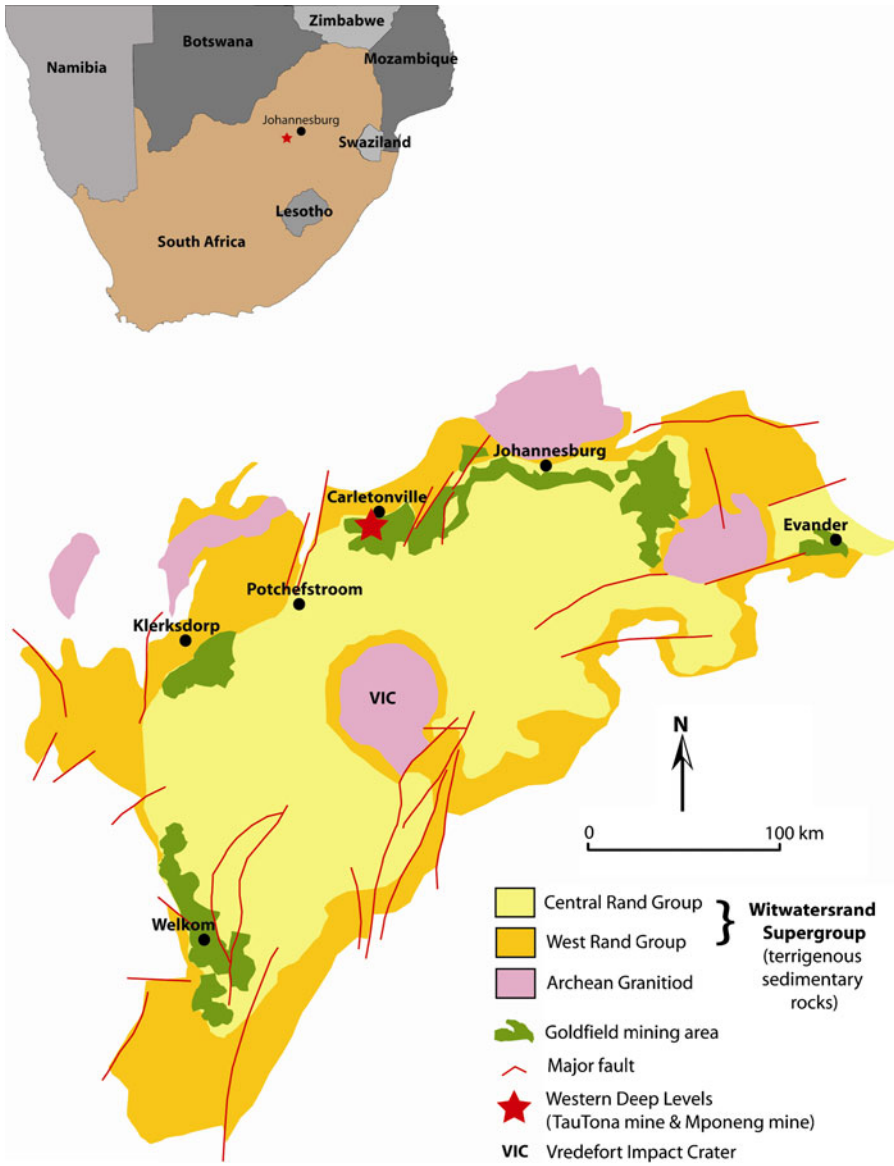

Figure 1
Simplified geological map of the Witwatersrand Basin, South Africa, illustrating the distribution of the Witwatersrand Supergroup and the Archaean Granitoid. Major goldfields (*green*) and the location of the TauTona and Mponeng mine in Western Deep Levels are marked (after Frimmel and Minter, 2002)

rifting, the basin underwent low-grade burial metamorphism up to lower greenschist grades (Robb *et al.*, 1997). Peak metamorphism coincided with the emplacement of the mafic and ultramafic Bushveld intrusion at 2,050 Ma (Robb *et al.*, 1997). This resulted in major thermal perturbations of the basin. The Vredefort meteorite impact at 2,024 Ma (Kamo *et al.*, 1996) was followed by a significant uplift of the basin and a retrograde overprint of the metamorphism. Eroded and uplifted structures were the provenance of the younger ($\sim$200 Ma) Karoo sequence, composed mainly of interbedded shale and sandstone layers, only a few hundred meters thick (Ward *et al.*, 2004). Since the Vredefort impact, the Witwatersrand Basin has been tectonically inactive, and subjected to extensive erosion that is

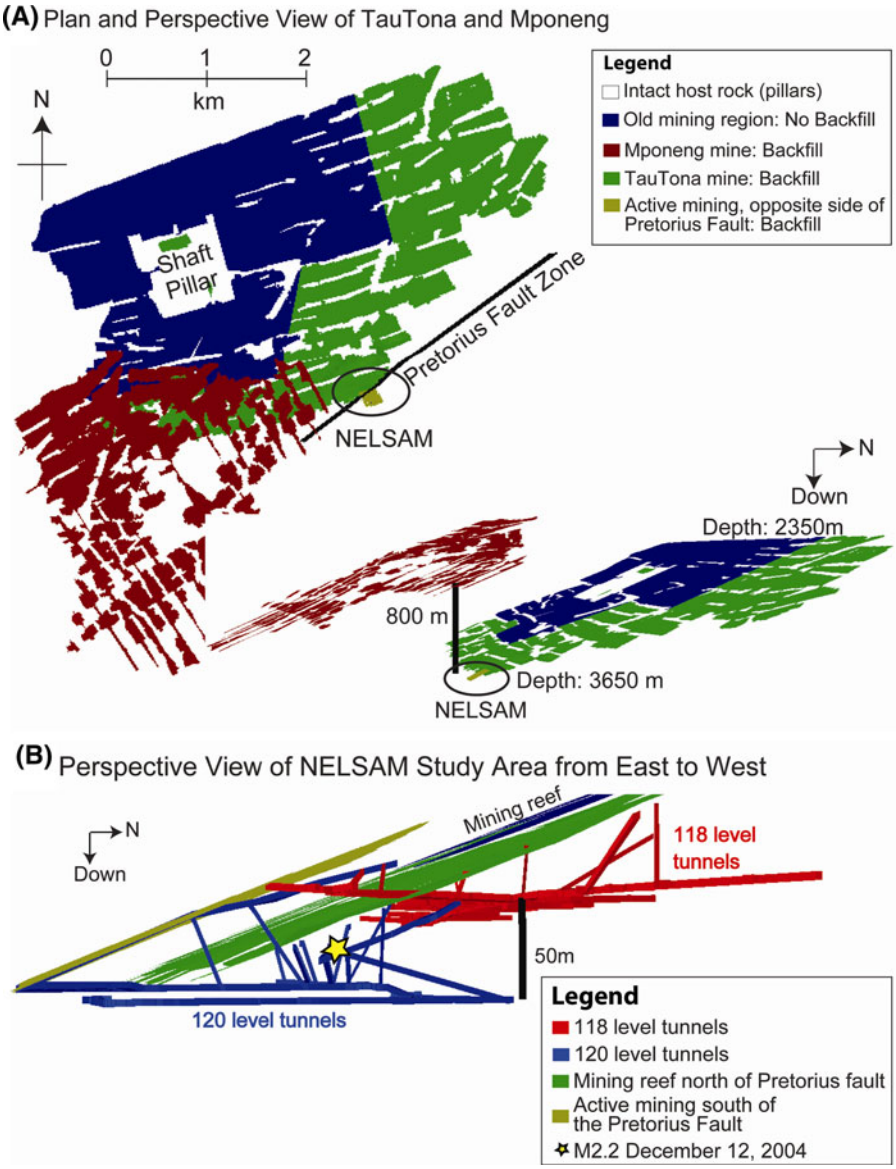

Figure 2

Layout of the TauTona mine, South Africa (after Lucier *et al.*, 2009). **a** Plan view of the mining at Mponeng mine (*brown*) and TauTona mine (*blue* and *green*) and the Pretorius fault (*black*). The *colored regions* are mined areas, and the *uncolored regions* are un-mined, intact rock left as pillars. The NELSAM research site is marked in the south eastern part of TauTona mine. The 3D view of the mining reef from the east in the lower left; the NELSAM site is marked; Pretorius fault not shown. The TauTona mine produces mainly from the Carbon Leader Reef which is about 800 m stratigraphically below the Ventersdorp Contact Reef of Mponeng mine. **b** Perspective view of the NELSAM site (after Lucier *et al.*, 2009). The currently active mining (*yellow*) is offset relative to the older mining (*green*) by the ~30 m throw along the Pretorius fault. The level 118 (*red*) and level 120 (*blue*) tunnels are separated by ~60 m. The M2.2 rupture of December 12, 2004 (*yellow star*) is located ~20 m below the mining reef

estimated to be between 5 and 10 km (McCarthy *et al.*, 1990).

The gold mineralization is mainly concentrated within conglomerate horizons of the West Rand and Central Rand Groups, often accompanied with hydrocarbon (Frimmel and Minter, 2002). The TauTona mine is located on the northern margin of the Witwatersrand Basin (Fig. 1) where the metamorphosed

sedimentary rocks of the West and Central Rand Group are tilted 20°–25° to the SSE. The mining horizons in this mine, are the Carbon Leader Reef, down to depth of 3.6 km; and the Ventersdorp Contact Reef, about 800 m stratigraphically above the Carbon leader Reef, which is also mined in the overlapped Mponeng mine (Fig. 2a). The mining is generally performed using the 'long-wall' method (BRADY and BROWN, 1993) of following the gold-bearing horizons leaving unmined areas as support pillars in Fig. 2a.

3.2. The Pretorius Fault

The NELSAM site is located at the south side of the TauTona mine, where the mining horizon is displaced vertically $\sim$30 m by the Pretorius fault (Fig. 2b). Most of the area north of the fault was mined in the long-wall method with backfill for support (GRICE, 1998). The unmined areas south of the Pretorius fault are future reserves to be mined down to depth of more than 4 km. Figure 3 displays the tunnel layout map within the NELSAM site. Note that all mining levels are projected on top of each other on a map view. Red lines trace tunnels at 118 level and blue lines trace tunnels at level 120. The mined reef follows an inclined surface that dips to the SSE (gray in Fig. 3).

The Pretorius fault is about 10 km long and trends in ENE direction. The fault forms a sub-vertical zone and extends from about 1 km to at least 5 km below the surface and is exposed in the TauTona mine at a depth of 3.6 km, and Mponeng mine at depth of 2.8 km (GIBSON *et al.*, 2000a). Underground mapping suggests that the Pretorius fault is an oblique right-lateral fault with horizontal displacement of about 200 m and vertical displacement, south side thrown up, up to 100 m (D. KERSHAW, personal communication, 2005) and up to 30 m at the NELSAM site. In TauTona mine, the Pretorius fault crosscuts quartzitic rocks of the Lower Johannesburg Subgroup of the Lower Central Rand Group (FRIMMEL and MINTER, 2002). The layers include fine to very coarse grained quartzite that range in color from light to dark gray. In the NELSAM site a mafic dike, called Swannie dike, with a thickness up to 60 m is exposed along the south side of the fault-zone. In the Mponeng mine, the Pretorius fault crosscuts quartzitic rocks from the Venterspost Formation at the bottom of the Ventersdorp Supergroup, overlain by metabasalt of the Klipriviersberg Group (FRIMMEL and MINTER, 2002).

3.3. Seismic Activity Along the Pretorius Fault

The seismic network in TauTona mine was developed and maintained by ISS International (VAN ASWEGEN and BUTLER, 1993). This is a dynamic network with a few tens of seismometers at $\sim$0.5 km spacing stationed primarily in the reef level in a quasi two-dimensional distribution. The M2.2 event triggered 16 seismometers of the ISS network that assigned to it a moment of 2.6×10^{12} Nm and radiation energy of 3.0×10^{7} J (BOETTCHER *et al.*, 2006). Recent analysis of the ISS catalog relocated several events of $M > 2$ and placed them closer to the Pretorius fault including the 2004 M2.2 event (Fig. 4a) (BOETTCHER *et al.*, 2006, 2009). The exposed rupture-zone of this event is located within the Pretorius fault-zone and $\sim$120 m away from the hypocenter determined by the ISS seismic network (Fig. 4a). The apparent location difference is probably due to the large spacing of seismometers in the TauTona mine and their distribution.

Most of the M2.2 earthquake damage was located in the tunnels 120-17-raise, 120-17-a and 120-17-b (Fig. 4b). Major damage occurred along 70 m in the 120-17 tunnel (Fig. 4b) that was closed down due to safety hazards. Several nearby tunnels suffered minor damage as reported by the miners. The rupture-zone itself is exposed at the intersection of the 120-17-raise and 120-17-b tunnel (Fig. 4b), as identified immediately after the M2.2 December 12, 2004 event. Six months after the event, in June 2005, a second tunnel (120-MM-incline) was developed east of the lateral extension of the rupture-zone, oblique to the 120-17-b tunnel. This new tunnel was excavated across the rupture-zone and allowed us to extend our mapping into an area that was not cut by a tunnel before the event. Similar approach was practiced by Gay and Ortlepp (1979) and Ortlepp (2000) who mined their way into the rupture zones.

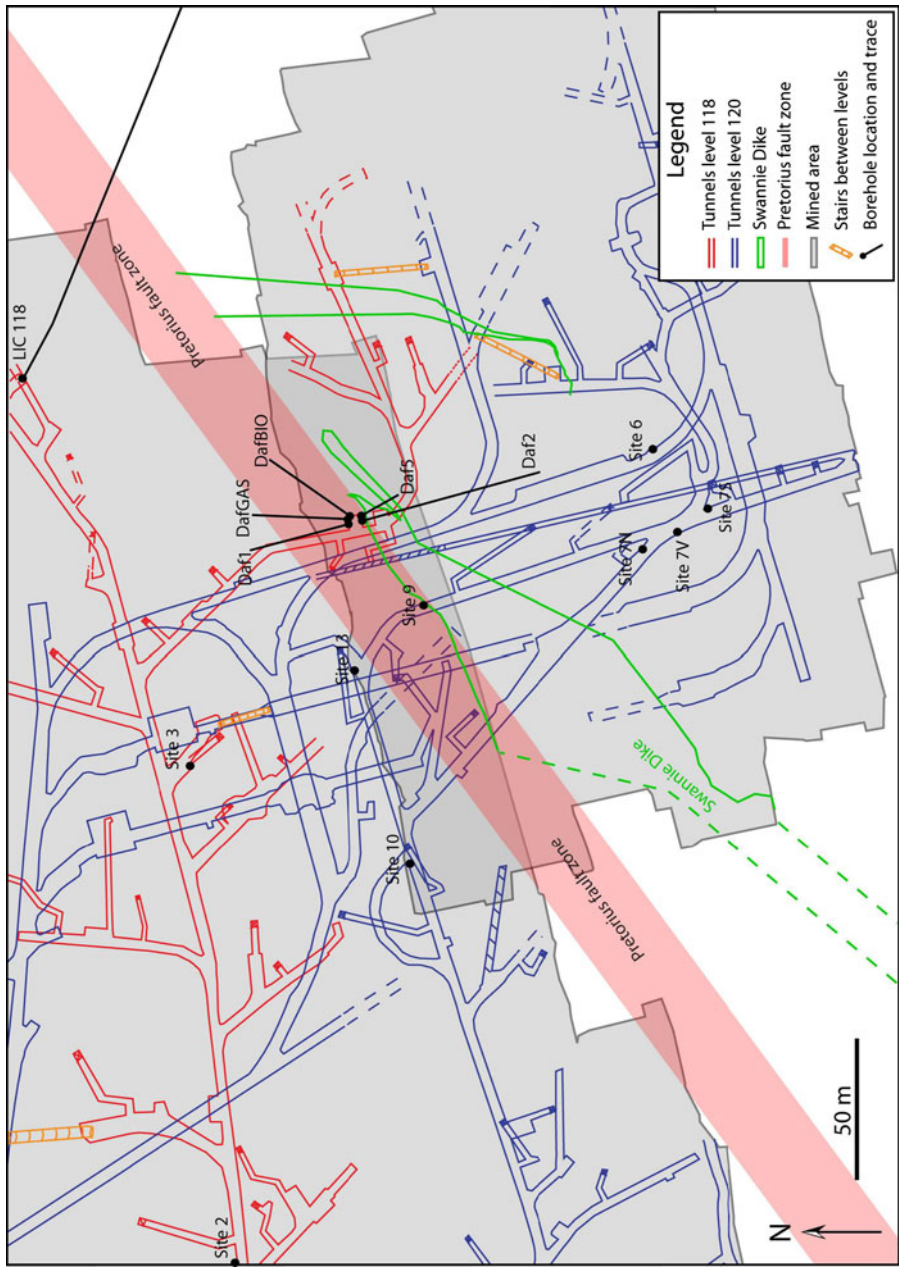

Figure 3
Map view of the NELSAM site, TauTona mine, South Africa. Tunnels of level 118 (*red*) and level 120 (*blue*) are projected on *top* of each other. The mined reef (*gray*) dips 20–25° to the SSE and is offset by the Pretorius fault. The marked boreholes include *vertical* holes 2 and 3 at level 118; *vertical* boreholes 6, 7 V, 9, 10 and 13 are at level 120; inclined boreholes Daf1, Daf2, DafGAS, DafBIO and Daf5 were drilled at level 118. LIC118 is a sub-horizontal exploration borehole, drilled at level 118, which extends 900 m far away from active mining activities

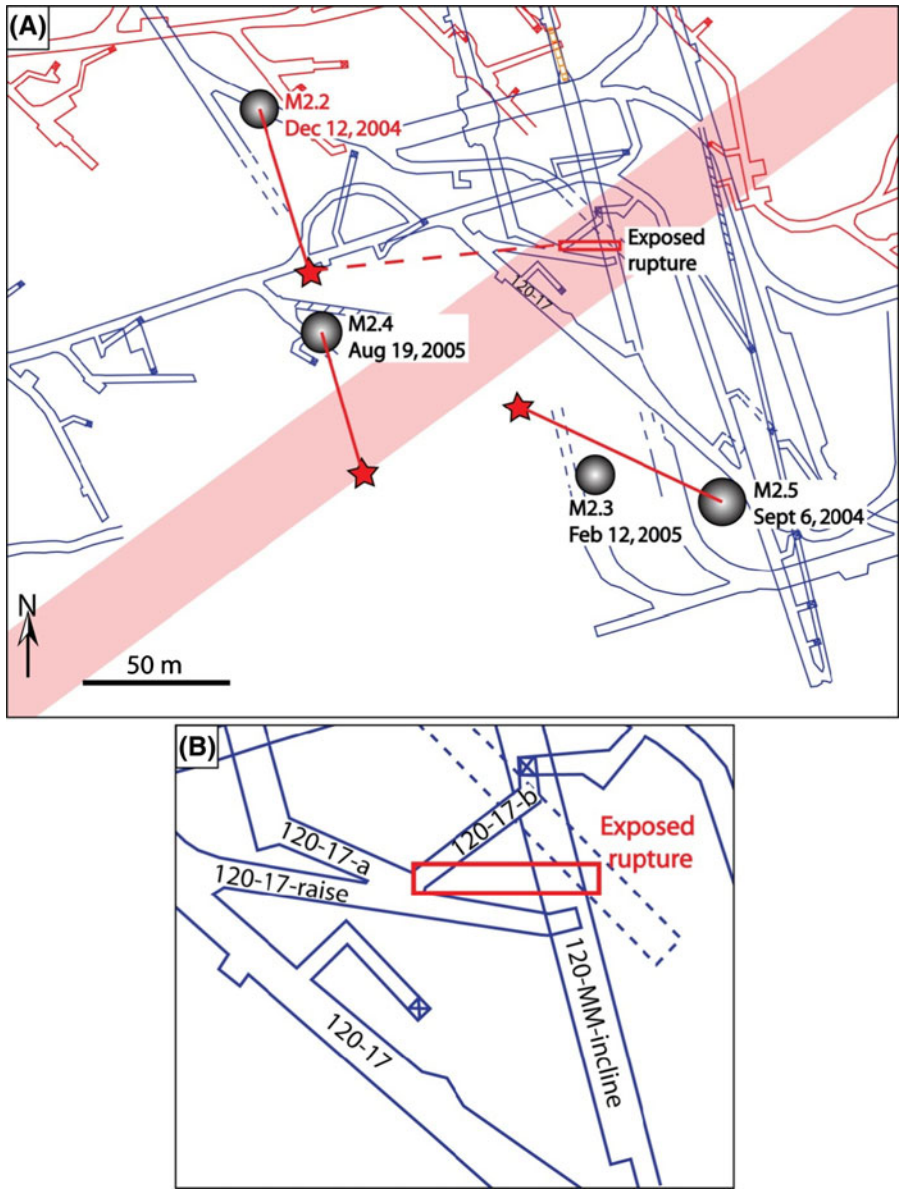

Figure 4
Region of the 2004, M2.2 earthquake and the NELSAM site. **a** Locations of events $M > 2$ that occurred since January 2004. *Circles* hypocenters by ISS network; *stars* relocated events by Boettcher *et al*. (2006). **b** Tunnel network at the proximity of the exposed rupture (marked in *red*). Tunnel 120-17-raise, 120-17-a and 120-17-b tunnels, existed before the event and tunnel 120-MM-inclined was developed 6 months after the M2.2 event

4. Internal Structure of the Pretorius Fault

4.1. Mapping Methods

We mapped the Pretorius fault-zone in seven tunnels that cut across the fault at depth of 3.5–3.6 km in TauTona mine. The typical height and width of these tunnels is ~3 m, and they are horizontal or inclined ~20°, subparallel to the bedding. We mapped at scales of 1:100 and 1:50, complemented by local mapping at 1:10 scale. A 4 m spacing grid was used for tunnel mapping at 1:100 and 1:50 scales, and a 10 × 10 cm wired grid for

1:10 scale. The 3D structure of the fault-zone is displayed by tunnel maps of the roof and both sidewalls with the sidewalls unfolded parallel to the roof-sidewall intersection (Figs. 5, 6).

The structure of the Pretorius fault-zone is presented in maps of three north–south trending tunnels (Fig. 5), and three inclined tunnels (Fig. 6); all these tunnel cross the fault-zone. The tunnels are labeled according to their depth and mining function. For example, tunnel 120-MM-incline (Fig. 5) denotes an inclined tunnel at depth of 12,000 ft, designed for men and material transport. In Fig. 5, the 120-MM-incline tunnel dips about 10°S, the 118-TW-Raise-120 slopes about 25°S, parallel to local bedding, and the 118-xcut is a horizontal tunnel. In Fig. 6, the 120-17-raise tunnel dips ~25° to the E, the 120-17-a and 120-17-b tunnels are horizontal.

4.2. Fault Segments

The Pretorius fault-zone is a composite structure with tens of segments that form a 25–35 m wide, sub-vertical zone. The segments form an anastomosing network of dominantly east–west striking, moderate to steeply dipping (40°–90°), quasi-planar faults that crosscut and intersect each other. Three main types of segments were identified in the mapped tunnels: cataclasite-bearing fault segments, fault-associated fractures and bedding-parallel fault surfaces. In the tunnel maps, the cataclasite segments are traced in green, fault-zone associated fractures in red, and bedding surfaces in blue (Figs. 5, 6).

4.2.1 Cataclasite-Bearing Segments

Structure Many of the individual segments in the fault-zone contain green to gray cataclastic rocks; their microstructure is described later. These segments are predominantly steep, dipping north and south with minor cases of bedding-parallel fault segments (green traces in Figs. 5, 6). The color of the cataclasite changes from green to gray towards the Swannie dike that bounds the Pretorius fault-zone on the south (Fig. 5, 120-MM-incline tunnel). We did not observe offsets of crosscutting segments. Dominantly south dipping segments with abundant bedding surfaces are observed within the three

Figure 5
Structural tunnel maps of the Pretorius fault at the NELSAM site. The tunnel maps display three mapped panels, central one for the roof and the two others for the sidewalls. The 120-MM-incline tunnel is inclined ~20° to the S, 5 m wide and 5 m high and mapped at a scale of 1:100. The 118-TW-Raise-120 is inclined ~20° to the N, the 118-xcut tunnel is horizontal; both are ~3 m wide and ~3 m high, and were mapped at a scale of 1:50. Cataclasite bearing fault segments (up to 50 cm thick) are traced by *green* and *gray lines*, fractures in *red*, bedding surfaces in *blue* and quartz veins in *yellow*. The principal-slip-zone (*PSZ*) is linked between the three tunnel maps (see text for details). The segments that are reactivated by the M2.2 of December 12, 2004 are traced in *light green*

tunnels (Fig. 6), most of which are on the northern side of the Pretorius fault-zone. Fault segments within the 118-xcut tunnel (Fig. 5) display two sets of south and north dipping segments with mean values of 69°/170° ± 17° (T1 in Fig. 7) and 72°/346° ± 9° (T2 in Fig. 7). The 39° angle between these two sets suggests that they belong to a conjugate set.

We found a distinct difference between the north and the south side of the Pretorius fault-zone (Fig. 5). Within the north side, bedding surfaces are abundant and the quartzitic host rock is light gray. On the south side, bedding surfaces are not observed and the density of cataclasite-bearing segments is significantly larger. Occasionally quartz veins are observed within the south section of the fault-zone (yellow line in Fig. 5). The dark gray quartzitic rocks on the south side are the up-thrown quartzites of lower stratigraphic horizons (Rob Barnett, personal communication, 2007).

The transition from the north and south side of the Pretorius fault-zone occurs along one dominant fault segment (Fig. 5). We regard this segment as the principal slip zone (PSZ) that accommodated most of the ancient slip of the fault, whereas the surrounding segments and fractures are part of a wide damage zone with smaller amount of slip. The PSZ is best exposed in the 120-MM-incline tunnel (Figs. 5, 8) where its features are:

1. Sub-vertical segment, dipping 81° to the south with a dark green cataclasite zone of 30–50 cm thick (Fig. 8).
2. As described above, the PSZ divides between the northern blocks of light gray quartzite rock with

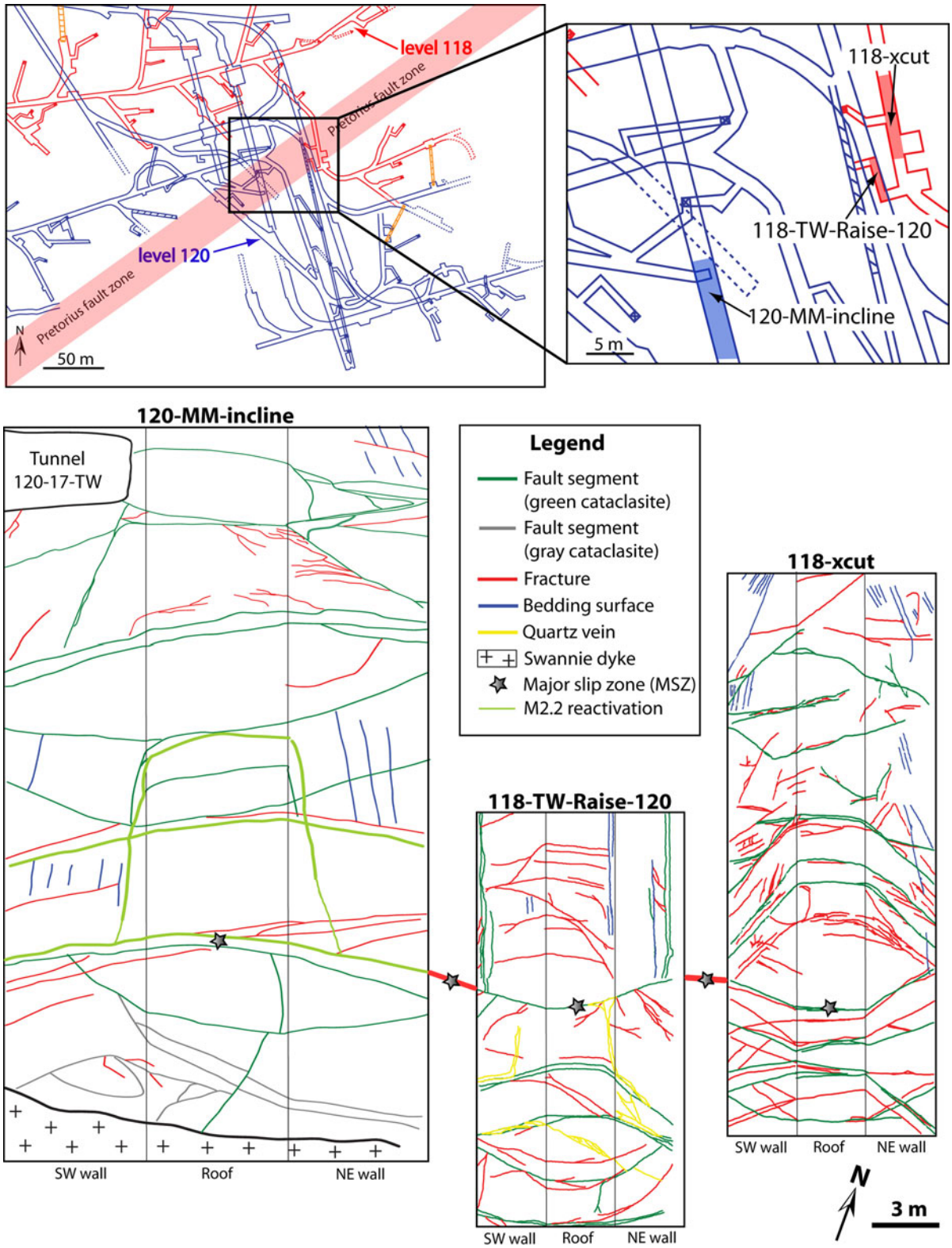
level 118
Pretorius fault zone
level 120
Pretorius fault zone
N
50 m
118-xcut
118-TW-Raise-120
120-MM-incline
5 m
120-MM-incline
Tunnel
120-17-TW
SW wall
Roof
NE wall
Legend
Fault segment
(green cataclasite)
Fault segment
(gray cataclasite)
Fracture
Bedding surface
Quartz vein
Swannie dyke
Major slip zone (MSZ)
M2.2 reactivation
118-TW-Raise-120
SW wall
Roof
NE wall
118-xcut
SW wall
Roof
NE wall
N
3 m

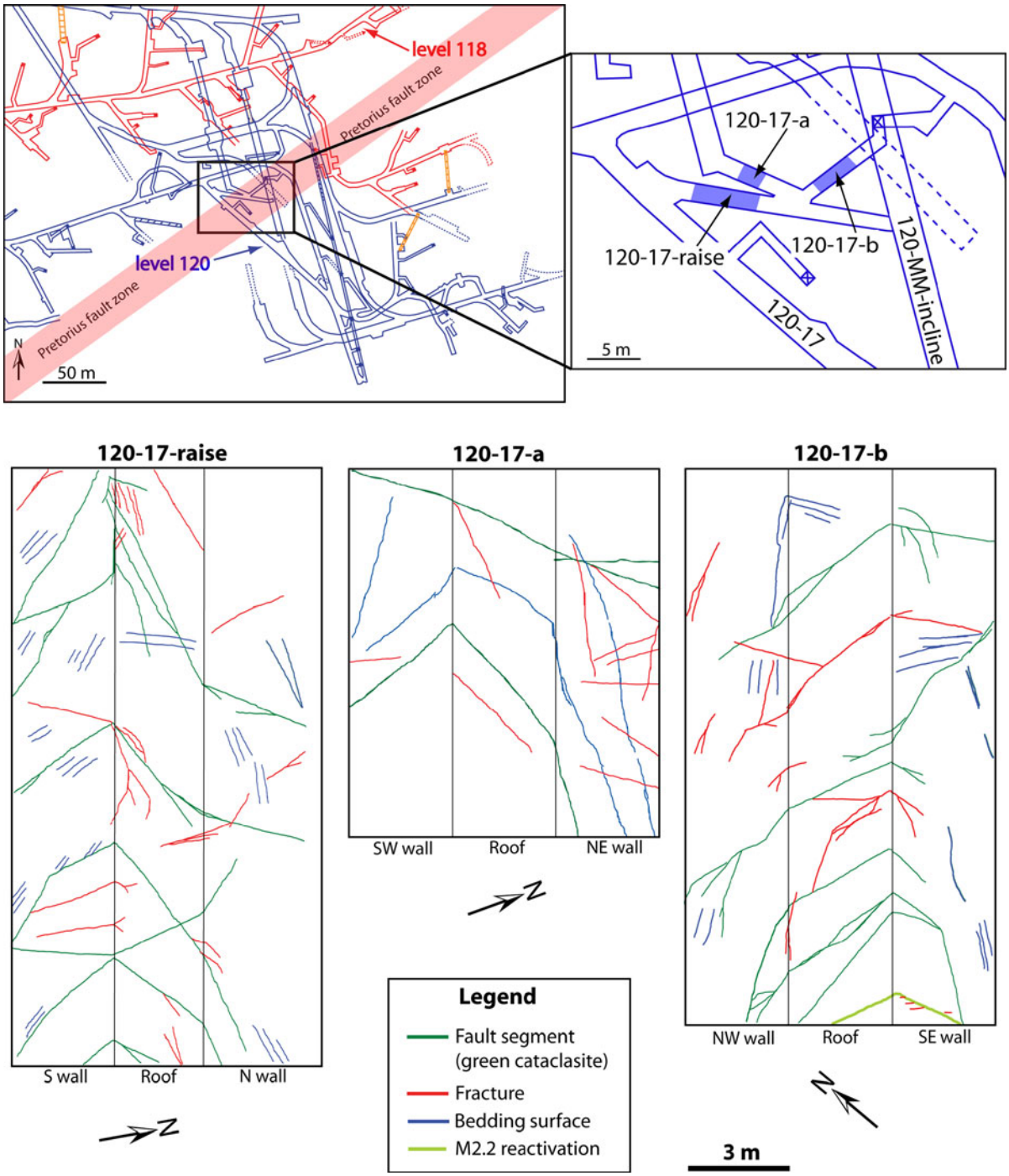

Figure 6
Structural tunnel maps of the Pretorius fault at the proximity of the M2.2 of December 12, 2004. The 120-17-raise tunnel dips ~25° to the E, the 120-17-a and 120-17-b tunnels are horizontal. All three tunnels are ~3 m high and ~3 m wide and were mapped at a scale of 1:50. Legend as in Fig. 5

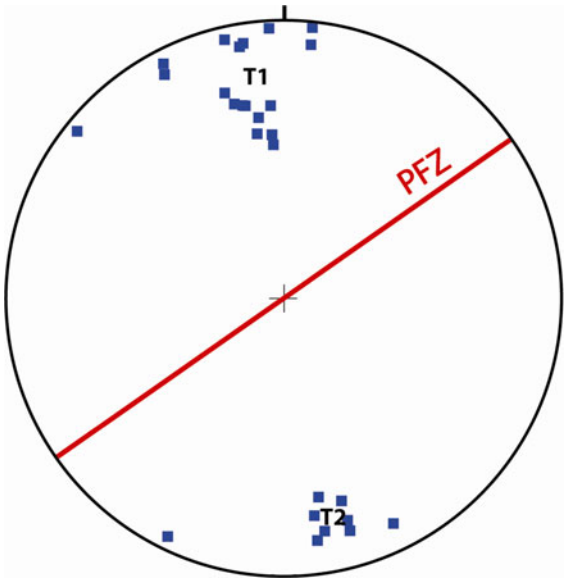

Figure 7
Stereographic projection of poles of fault segments in 118-xcut tunnel (fault maps in Fig. 5). The two fault sets are oriented 69°/170° ± 17° and 72°/346° ± 9°

abundant bedding surfaces, and the southern block of dark gray quartzite and higher density of cataclasite-bearing fault segments (Fig. 5).

3. Light green to yellow cataclasite developed along the PSZ edge during ancient reactivation of the PSZ (Fig. 8 and discussion below).
4. Recent reactivation during the M2.2 event on December 12, 2004, recognized by white fresh rock powder that dominates along the contact between the cataclasite and quartzite (Fig. 8); This fresh rock powder is interpreted to be generated during co-seismic slip; detailed descriptions appear below.

Similar features along one dominant segment, which we regard as the continuation of PSZ, are observed in the 118-TW-Raise-120 and 118-xcut tunnels, with the addition of quartz veins that are observed on the south of this segment (Fig. 5). The cataclastic zone here is up to 30 cm thick, and bedding-parallel injection of cataclasite are observed from this segment (118-TW-Raise-120 Fig. 5), with the injected cataclasite being up to 20 cm thick and continuous for several meters. These segments are interpreted as linked to the PSZ in the 120-MM-incline (Fig. 5), indicating alternating N and S inclinations of the steep PSZ.

Two sets of slickenside striations were observed locally along several segments of the Pretorius fault-zone. The most dominant and best developed set indicates a sub-horizontal right-lateral strike-slip motion. The orientation of this slickenside set corresponds with the ancient strike-slip motion along the Pretorius fault. A second set of slickenside striations includes a poorly developed, sub-vertical group of slickensides. No cross-cutting relations between both slickenside sets could be established. The existence of two distinct sets of slickensides suggests that the total oblique right-lateral slip along the Pretorius fault is a result of either two separate tectonic events or slip-partitioning between lateral and vertical motion during the same tectonic phase.

Multiple slip stages The PSZ of the fault-zone displays two cataclasite bodies that can be differentiated by their color (Fig. 8); we interpret these bodies as indicating two separate slip stages of unknown magnitude. A dark-green cataclasite body is interpreted as forming first, and a lighter green cataclasite body, which appears along the dark-green cataclasite and locally cross-cut it, is interpreted as a second stage. The light-green cataclasite segments (green in Fig. 8) are at an angle of 15°–20° with respect to the PSZ and are interpreted as Riedel shears associated with ancient slip in which the north block of the fault moved upward with respect to the south block (schematic drawing right side of Fig. 8). Gibson *et al.* (2000a) suggested that the Pretorius fault was reactivated by gravitational collapse and extension during the Platberg rifting and/or the Vredefort impact. The features in Fig. 8 could be the related to one of these phases.

4.2.2 Fracture Networks

Borehole analysis The fractures of the Pretorius fault-zone were analyzed using image logs in 11 boreholes drilled at the NELSAM site (Reches, 2006; Lucier *et al.*, 2009). The boreholes were drilled from TauTona mine tunnels at levels 120 and 118, and boreholes were logged with a slim borehole Digital Optical Televiewer (DOPTV) made by Robertson Geologging, UK. Eight of the boreholes are 10 m deep, located within or close to the Pretorius fault-zone (borehole locations in Fig. 4). Six of the

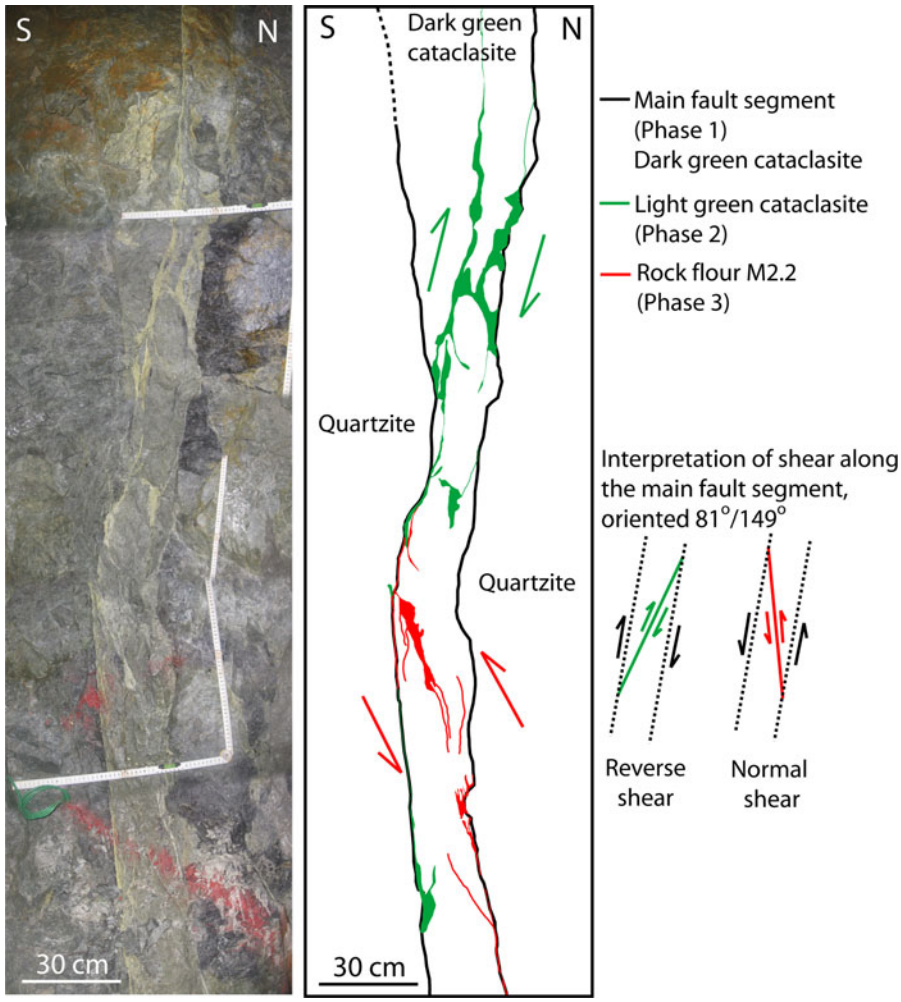

Figure 8
Details of the principal slip zone (*PSZ*) of the Pretorius fault in 120-MM-incline tunnel (location in Fig. 5), *left* photograph of the zone; *center line* drawing of the main structural features; *right* schematic presentation of the motion phases (*text*). The PSZ displays here three phases of activity: (1) formation of *dark-green* cataclasite; (2) formation of *light-green* cataclasite that cuts phase 1 cataclasite in a right-lateral Riedel shear fracture (*inset*); and (3) formation of a rock-flour zone during the M2.2 event (details in *text*)

boreholes are vertical (site 2, 3, 7 V, 9, 10 and 13) and two are inclined 45° to azimuths 152° (site 7 N) and 323° (site 7S). All these boreholes are 75 mm in diameter. Three 20–50 m deep holes are drilled at 20°, sub-parallel to bedding, at azimuths of 165°, 150° and 36°, respectively, with a diameter of 96 mm (boreholes marked Daf2, Daf5 and DafBio). These three holes cross the Pretorius fault-zone. The different inclinations and range of azimuths of the boreholes is likely to eliminate a bias in fracture orientation sampling.

The Digital Optical Televiewer records an oriented image of the borehole wall with a radial resolution of 720 pixels per revolution and a vertical resolution up to 1 mm. Borehole features were identified with RG-DIP interpretation software version V6.2 by Robertson Geologging. The software calculates the true fracture orientations and corrects for the borehole orientation and magnetic declination. In most boreholes, the images are of good to excellent quality; boreholes Daf2, DafBio and hole 13 have poor quality images due to logging difficulties.

Fracture orientations We identified three types of features in the borehole images: (1) bedding surfaces; (2) fractures with complete, continuous curves; and (3) fractures with partial or discontinuous trace across

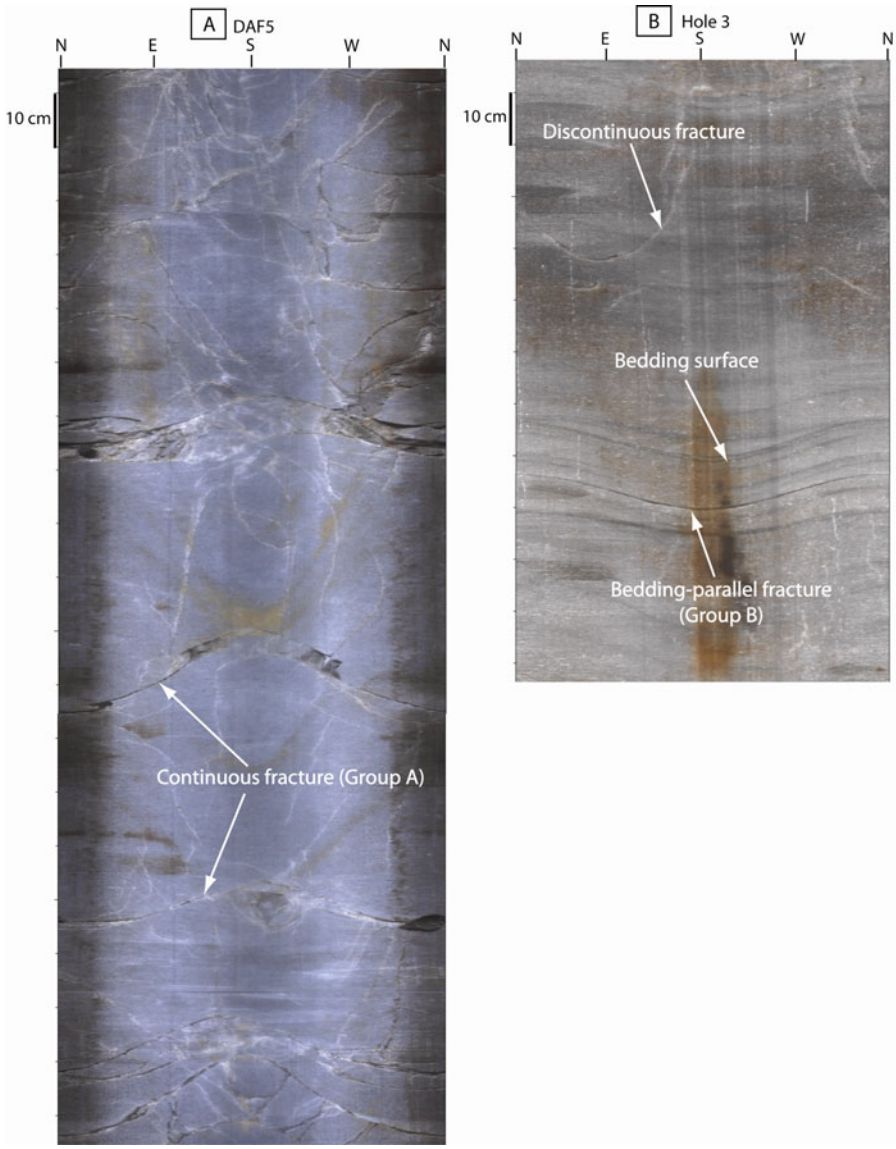

Figure 9
Partial sections of the borehole image logs. **a** Image log from borehole drilled across the Pretorius fault-zone sub-parallel to bedding and plunging 20° towards 150° (DAF5 in Fig. 4). Note high fracture density (set A in text). **b** Image log of borehole #3 away from the fault-zone (location in Fig. 4); note smooth dark bedding surfaces, rough bedding-parallel fractures, and discontinuous fractures (*partial curves*)

the image (Fig. 9). Bedding-parallel fractures were distinguished from bedding surfaces by the presence of roughness and irregularities, whereas bedding surfaces appear as smooth, dark gray features (Fig. 9). Cataclasite layers could be recognized in few cases.

The orientation data of the fractures and bedding surfaces in the 11 boreholes is displayed in Fig. 10. Density contours on the continuous fracture dataset indicate three dominant sets of fractures, marked A, B and C in Fig. 10c. These fracture sets are oriented 66°/139° ± 12°, 30°/169° ± 14°, and 06°/120° ± 12°, respectively. Fracture set B is interpreted as bedding-parallel fractures, as bedding surfaces from all 11 boreholes have an average orientation of 28°/171° ± 12° (Fig. 10d). While the discontinuous fractures display more scatter, they appear to belong to the same fracture population of the continuous fractures (Fig. 10a, b).

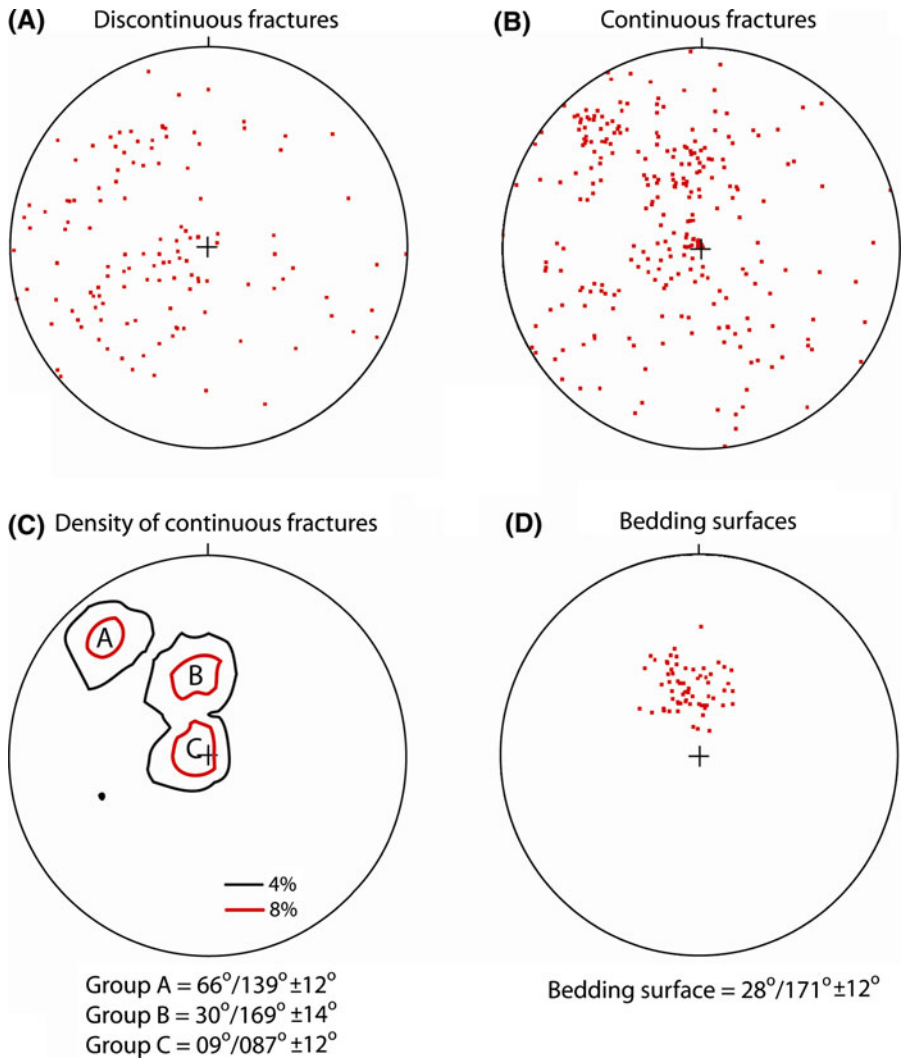

Figure 10
Orientations of fractures and bedding surfaces mapped on image logs of 11 boreholes within the NELSAM site (lower hemisphere stereographic projection). **a** Discontinuous fractures. **b** Continuous fractures; note pattern similarity with (**a**). **c** Density contours of the continuous fractures with identified sets *A*–*C*. **d** Bedding surfaces, sub-parallel to set *B*

Figure 11 shows fracture orientations in individual boreholes that are grouped according to location with respect to the fault-zone. The figure includes fracture density, $f =$ [number of fractures]/[image log length], and the distance of the borehole from the fault-zone, d. The boreholes north of the fault-zone (Fig. 11a) display predominance of bedding-parallel fractures of set B. This set, however, is poorly developed south of the fault-zone (Fig. 11c), and absent in boreholes drilled within the fault-zone (Fig. 11b). Fractures of set A are dominant within Daf5, inside the fault-zone but are almost absent outside the fault-zone. Fractures of set C are only present in boreholes Daf5 and borehole 13.

In summary, the fractures associated with the Pretorius fault-zone are dominated by set A, 66°/139° ± 12° within the fault-zone, bedding-parallel fractures (set B, 30°/169° ± 14°) occurs mainly outside and north of the Pretorius fault, where almost no other fractures were observed. Fractures of set C (06°/120°) occur both inside and outside the fault-zone. The origin of these fracture sets is discussed later.

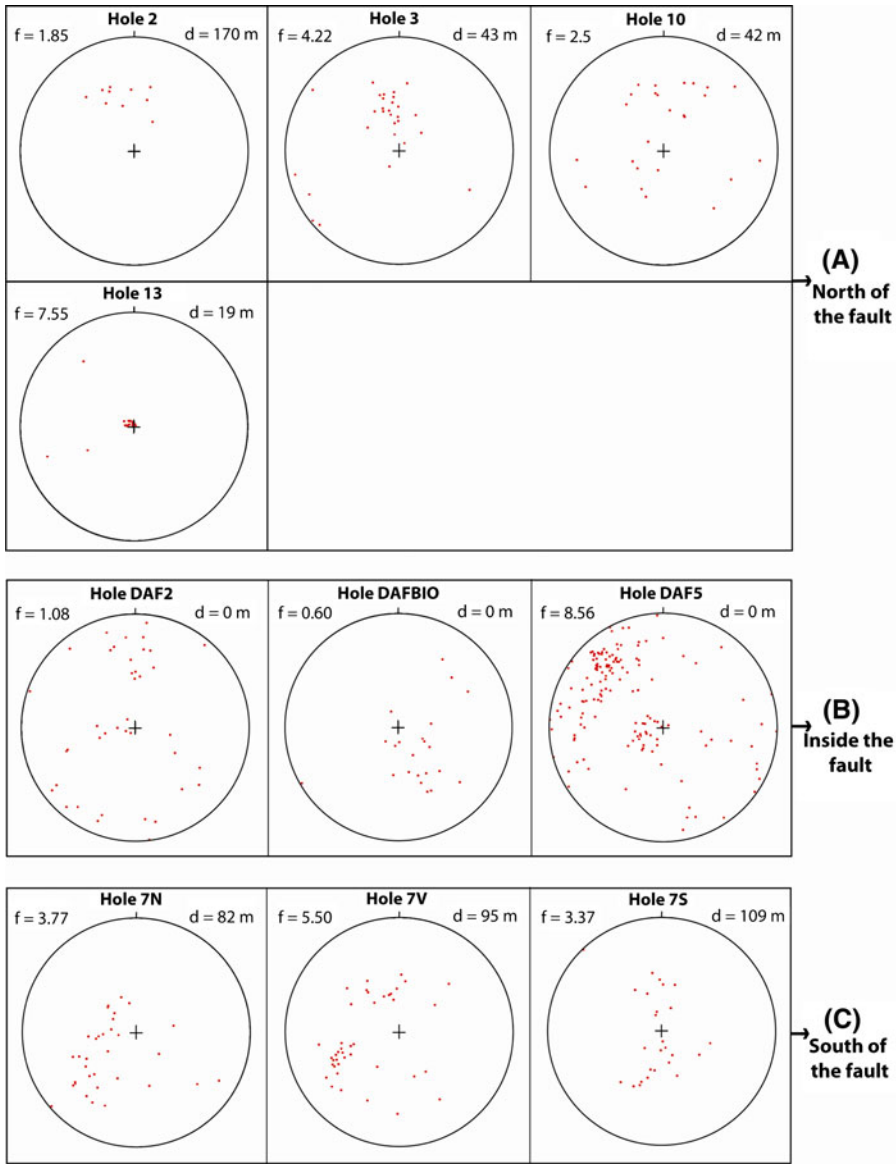

Figure 11

Fracture orientations mapped in the individual borehole within the NELSAM site (lower hemisphere stereographic projection). Borehole locations in Fig. 3. Each *plot* shows the fracture density, f, which is the [number of fractures]/[drilling length in m], and the distance d, of the borehole from the center of the Pretorius fault-zone. **a** Fracture orientations north of the fault-zone; note the dominance of set *B*. **b** Fracture orientations within the fault-zone; note high fracture density in DAF5 with dominance of set *A*. **c**. Fracture orientations south of the fault-one; note the scattered pattern of fractures

5. *Fault Rocks of the Pretorius Fault*

5.1. *Field Appearance*

Many of the segments in the Pretorius fault-zone are recognized by a highly cohesive cataclasite that is distributed along fault segments in planar zones with sharp, quasi-planar contacts within the host rock (Figs. 8, 12). The cataclasites occur in three distinct colors: dark-green, light-green–yellow, and gray; the latter is found only in the vicinity of the Swannie dike on the south side of the fault-zone (Figs. 5; 6). Based on the cross-cutting relations described above, it is

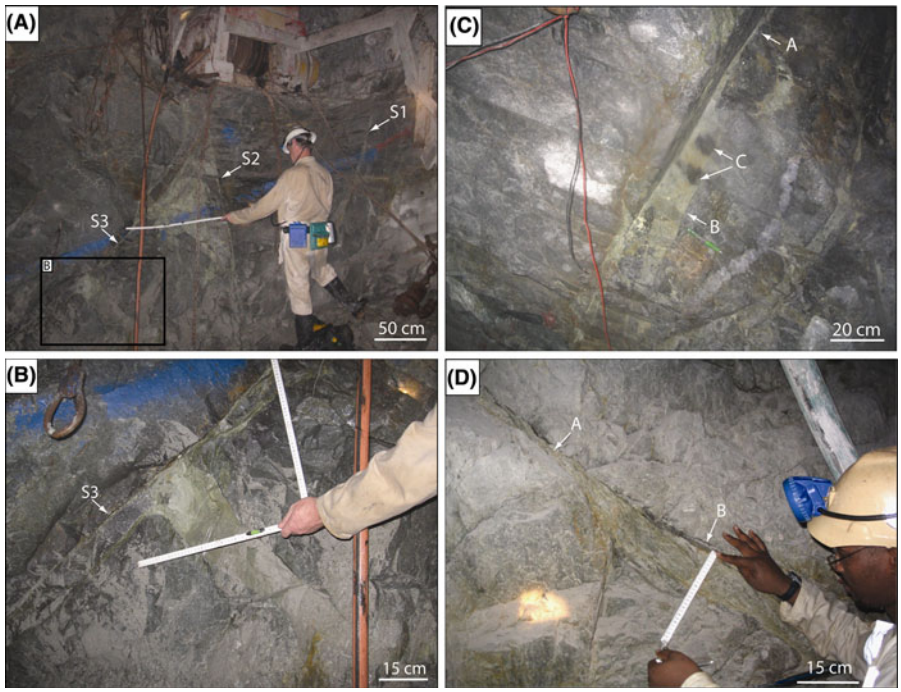

Figure 12
Cataclasite carrying fault segments in the Pretorius fault-zone, NELSAM site. **a** Two steep fault segments with cataclasite zones up to only a few mm thick that dip in opposite directions (S1 and S2), and a bedding-parallel fault segment (S3); location120-MM-incline. **b** An injection vein up to 15 cm thick injected into the quartzite from the S3 fault segment, with a cataclastic zone of just a few mm. **c** A cataclasite zone with 1–18 cm thickness variations; note quartzite clasts up to 12 cm in size at *C*; location 118-xcut. **d** A cataclasite zone with thickness variations from 2 cm at *A* to 11 cm at *B*; location 118-xcut

likely that the different colors represent different activity stages. Figure 12a illustrates two steep fault segments that dip in opposite direction (S1 and S2) together with a third segment that is parallel to the bedding (S3). The thickness the cataclasite zones along these three segments may vary profoundly even along a single segment, and it changes from a few mm to a few tens of cm over short distances of a few meters or less (Fig. 12). For example, along strike thickness variation is illustrated in Fig. 12c and d, from 1–2 cm at point A to 11–18 cm at point B. The thick zone of cataclasite is composed of sub-rounded massive quartz blocks up to 12 cm in size (C in Fig. 12c).

Cataclasite injection veins are common and they range in thickness from a few cm to tens of cm thick. For example, a cataclasite vein up to 15 cm thick was apparently injected from the bedding-parallel segment into the massive quartzite (Fig 12b). The majority of the veins are injected sub-perpendicular

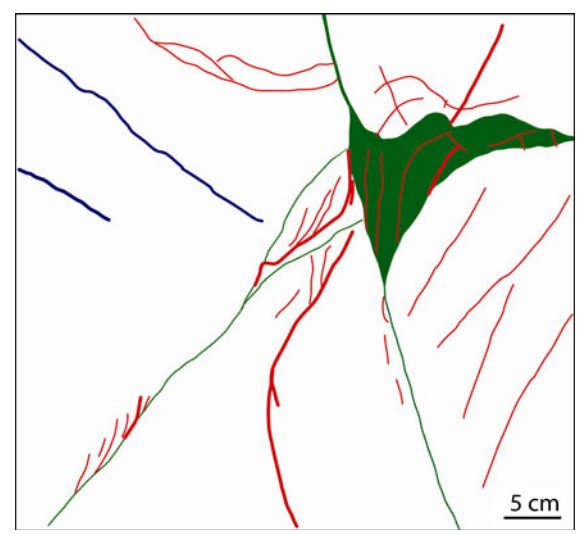

Figure 13
Map of an injection vein on the NE-wall of the 118-xcut tunnel; cataclasite in *green*, fractures in *red*, bedding surfaces in *blue*. The vein with maximum thickness of ~15 cm was injected from a fault segment with a cataclasite zone of only 1 cm thick

to fault segments (Figs. 12b; 13). Figure 13 represents a detailed map (scale 1:10) of an injection vein on the south side of the fault-zone. The injection has a maximum thickness of $\sim$15 cm and originated from a fault segment only 1 cm thick. Several large injection veins with thicknesses up to tens of cm have been injected along bedding surfaces, e.g., a vein on the north side of the fault-zone (Fig. 5, tunnel 118-TW-Raise-120). These bedding-parallel injection veins can be laterally continuous for a few meters.

The common appearance of injection veins and the intense thickness variations suggests that the cataclasite could flow during its formation. These features led to previous interpretation of the cataclasite zones as pseudotachylytes (Killick *et al*., 1988), but this interpretation is not supported by our microstructural analysis (below) which led us to interpret the present-day cohesive cataclasite as gouge that was incohesive and could flow at the time of its formation.

5.1.1 Microstructure

We examined the cataclasite microstructure in thin sections and SEM images (Zechmeister *et al*., 2005). The dark-green cataclasite is predominantly composed of ultra-fine grained matrix of quartz, mica, and opaque minerals and abundance of coarse, angular to rounded lithic quartzite fragments (Fig. 14a). The fragments range from less than a millimeter to tens of centimeters. An anastomosing cleavage locally appears within the matrix, surrounding the fragments (Fig. 14a). Some quartz fragments were dynamically recrystallized (marked P and D in Fig. 14a). Cataclasite flow structures are recognized by banding parallel and close to the fault segment wall, predominantly within the injection veins (Fig. 14b). The dark flow bands are composed of higher concentrations of mica while lighter bands are richer in quartz; the brown bands probably indicate oxidation (Fe?) (Fig. 14a). The SEM images of the dark-green cataclasite display very small grains down to micron-scale with local contacts between quartz grains that locally form curved structures of hourglass form (Fig. 15). As similar structures were associated with silicate crystallization in volcanic rocks (Anderson, 1991), we interpreted this observation to indicate sintering at grain contacts of granular material at elevated temperature (Zechmeister *et al*., 2005). The light-green cataclasite is less abundant in the fault-zone, generally forms thin zones up to tens of mm thick, along the edge of the dark-green cataclasite (Fig. 8). Its composition is similar to that of the dark-green cataclasite, but with less abundant and smaller quartz clasts.

The gray cataclasite is dominantly grain supported with a gray, ultra-fine matrix. The grains are composed of quartz with opaque minerals that are 0.005–1 mm in size. A brown oxidation zone appears between the grains. The grain size is reduced towards the contact of the cataclasite with the dike. By using an electron microprobe (EMP), we detected evidence for melting in a single sample of the gray cataclasite with microlitic textures referred to as 'snow flakes' (Zechmeister *et al*., 2005) (Fig. 16), which are interpreted as indicating a super-cooled melt (Lin, 1994; Swanson and Fenn, 1986). The origin of the fault rocks is discussed below. No evidence of such textures was found within the green cataclasites.

5.2. The M2.2 Rupture Zone

5.2.1 General Structure

The M2.2 earthquake of December 2004 reactivated at least three and possibly four segments of the Pretorius fault-zone. A general cross section through its rupture-zone (Fig. 17a) displays the reactivated segments, and the ancient structural features of the Pretorius fault-zone as mapped in the 120-MM-incline (Fig. 4b). A critical observation is the evidence for displacement during the M2.2 event. At two locations within the 120-17-TW, we found rock-bolts that were cross-cut and displaced by slip along the rupture zone (Fig. 18). The pre-rupture positions of the rock-bolts are recognized by a rusty imprint within the quartzite (details in Fig. 18b, c). The displacements are of 10 and 25 mm in a normal-dextral sense with a rake of 23° and 35°, respectively, along segment A, which is oriented 43°/167°. With no additional displacement data, we assume that the maximum slip of the M2.2 event was on the order of a few centimeters.

The reactivated segments were clearly identified by the presence of fresh, white, fine grained gouge

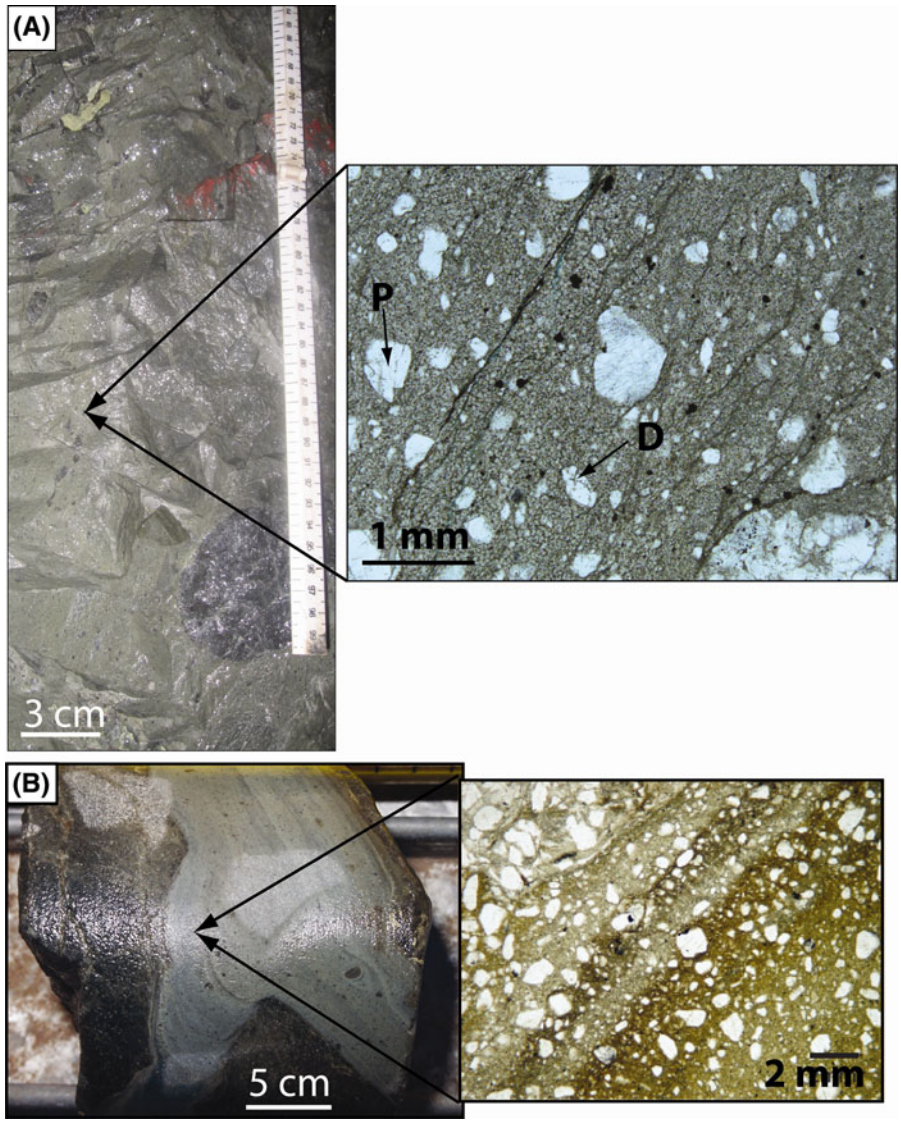

Figure 14

Dark green cataclasite of the Pretorius fault. **a** *Left in situ* view with a wide range of quartzite angular to rounded clasts; *right* a *thin* section (plane polarized) of the cataclasite with fine grained matrix, anastomosing cleavage, and quartz clasts; note dynamic re-crystallization of a few quartz clasts (*P* and *D*). **b** Cataclasite injection vein in the Pretorius fault. *Left* injection vein in a core section; *right thin* section (plane polarized) of this vein with flow banding parallel to its margins. The *dark bands* are mica rich zones

powder, referred to as 'rock-flour' that developed along the slip surfaces (Figs. 18, 19, 20). This rock-flour has been observed in almost all recent shear failures in the quartzitic rocks of South African mines (Gay and Ortlepp, 1979; Dor *et al*., 2001; Ortlepp, 2000; Stewart *et al*., 2001), and its presence is a reliable indicator of the shear motion in the mines. Further, we think that the ancient, cohesive cataclasite in the Pretorius fault, which was described above, was formed during Archaean tectonic actively of the fault in similar shear processes to the current rock-flour. Later, the cataclasite acquired its strength and cohesiveness by sintering and low-grade metamorphism (above).

We note that all four segments that slipped during the M2.2 event (marked A–D in Fig. 17) reactivated ancient segments of the Pretorius fault-zone. Further, reactivation occurred only along segments that carry

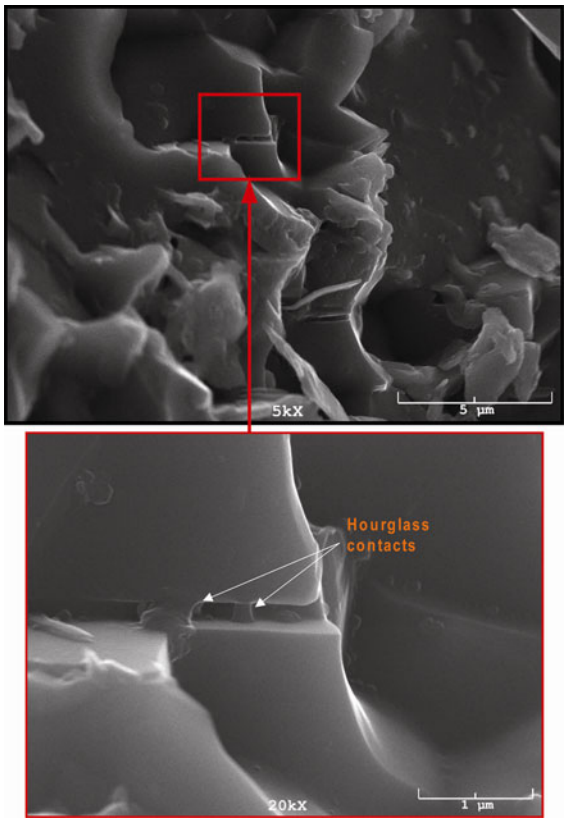

Figure 15
Scanning-electron-microscope images of cataclasite sample with fine-grains down to the micron-scale and hourglass contact between quartz grains (Zechmeister *et al.*, 2005); see text

cataclastic zones with thicknesses ranging from a few millimeters to tens of centimeters (Figs. 8, 18, 19, 20). Segment A is oriented 43°/167° (Figs. 17, 18a), and contains a 1–6 cm thick zone of cataclasite. Segment B is a bedding-parallel surface (Figs. 17, 19a, b) oriented 20°/161° that branches from surface A. Segment C, oriented 81°/149°, is the PSZ of the Pretorius fault-zone that was described above. Here, the cataclastic zone is up to 50 cm thick (Figs. 8, 17, 19c). In the tunnels, the rupture along segments A and B was mapped horizontally for 25 and 5 m vertically, and along segments C and D for ~6 m horizontally and ~5 m vertically.

Nearby tunnels, east and west of the exposed rupture-zone, do not display rupture surfaces, and thus bound the horizontal visible extent of the rupture-zone to 45 m. The mined reef, which is not accessible due to damage, is situated ~20 m above the exposed rupture surface and is regarded as a free surface that bounds the maximum vertical extents of the rupture-zone. This geometry bounds the maximum size of reactivated fault to ~3,400 m^2. Continuous exposures of the rupture-zone reveal a minimum area of 280 m^2. However, as the rupture-zone includes 3–4 segments in the same region (Fig. 17), the total area of the sheared surfaces is 2–3 times the minimum area. These upper and lower bounds of the exposed rupture-zone is in agreement with the estimated rupture area from the seismic signal which is 2,900 m^2 (Boettcher *et al.*, 2006).

5.2.2 *Slip Localization*

The slip of the M2.2 event reactivated existing segments of the Pretorius fault, and as indicated by the presence of 'rock-flour' (above), the slip was predominantly localized along the contacts between the cataclasite and the quartzitic host rocks (Figs. 8, and 18, 19, 20). The rock-flour may be distributed along both upper and lower contacts of the cataclasite zone (Fig. 19a). Segments A and B display 1–5 branching rock-flour zones, 0.5–1 mm thick each, along most of the exposure (Figs. 18, 19). In the exposed parts of segment A and B, the rock-flour zones did not cross-cut the 1–6 cm thick cataclasite zone.

The PSZ of the Pretorius fault-zone was also reactivated during the event (segment C Fig. 17). The PSZ consists of a 30–50 cm thick cataclasite with evidence for two phases of activity with corresponding dark green and light green cataclasite (above, Fig. 8). The slip during the M2.2 event of segment C is localized along the south-side contact between the cataclasite and the quartzite (Figs. 8, 19c), with about 1 mm thick rock-flour zone similar to segments A and B. An additional zone, which is up to 5 cm thick, of clay gouge appears along the south side contact (Fig. 19c), and at one location it crosses the cataclasite zone between south and north contacts (traced in red in Fig. 8). The orientation of this zone fits a Riedel shear fracture compatible with the normal slip during the M2.2 rupture (Figs. 8, 17), and we attribute it to this event.

The fourth reactivated segment, marked D in Figs. 17 and 20, is oriented 85°/340° with a 2–10 cm thick cataclasite zone. Similarly to the others, the slip

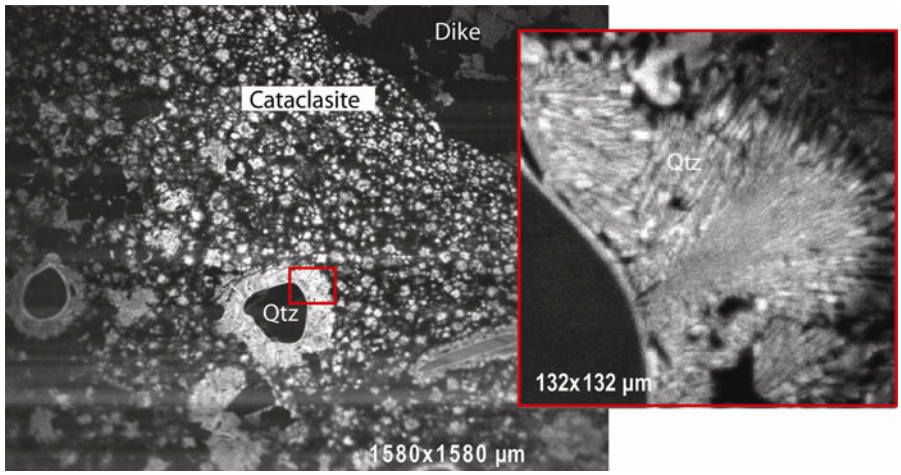

Figure 16
Electron microprobe images (Cathodeluminescence) of the gray cataclasite within a dike display microlitic textures ('snow flakes') around quartz grains suggestive of a super-cooled melt (Zechmeister *et al*., 2005)

was localized along the south contact of the cataclasite and the quartzite (Fig. 20) with a 1–2 mm thick rock-flour zone. The rock-flour along segment D was discovered at a later stage of the mapping, and it remains unclear if it was reactivated by the M2.2 event or later motion.

5.2.3 *Fresh, New Fractures Associated with the M2.2 Rupture*

In addition to the reactivation of pre-existing segments, the M2.2 event, it also generated some distinct fresh fracture systems. The most prominent one is a set of 5–7 sub-vertical fractures that branch away from segment A in the 120-17-TW tunnel, close to the site of the observed 25 mm of slip (above) (Fig. 21). Their position in the dilatational side of a normal fault (hanging wall), their sub-vertical orientation, and the presence of rock-flour along them suggest that they are mixed mode I-II fracture. Most likely, they propagated as wing-cracks (Reches, 1988; Reches and Lockner, 1994; Germanovich *et al*., 1994) in a direction normal to local tensile stress during the earthquake slip. We think that these fractures nucleated at the tip of the propagating rupture along segment A, and grew into the intact rock above it.

Another fresh fracture branches from segment B close to its intersection with segment C (PSZ) in the120-MM-incline. Here the pre-existing segment B is deflected, and it intersects segment C at almost a right angle (Figs. 17, 22). At this deflection, the rupture splits and one branch continues along the cataclasite-quartzite contact, and one branch forms a new quasi-planar shear fracture that extends up to segment C (Fig. 22a). This fracture widens locally to form a 1–2 cm wide shear zone with multiple secondary shear fractures (Fig. 22b).

5.2.4 *Main Features of the M2.2 Rupture-Zone*

The main structural features of the M2.2 rupture zone are list below, and their implications are discussed later:

1. The slip reactivated three or four, pre-existing large, quasi-planer segments of the Pretorius fault, that contain thick cataclasite zones (Fig. 8).
2. The reactivated segments are not parallel to each other (Fig. 17).
3. Slip, as identified by the presence of rock-flour, occurred almost exclusively along the contacts between the cataclasite and the host quartzitic rock (Figs. 8 and 18, 19, 20).
4. Locally, new, fresh fractures branched from the reactivated ancient segments and propagated up to 1 m into the intact quartzite. These fractures propagated either in mixed shear-tensile mode (Fig. 21) or shear mode (Figs. 8, 22).
5. The maximum observed shear displacement is 25 mm in oblique-normal slip.

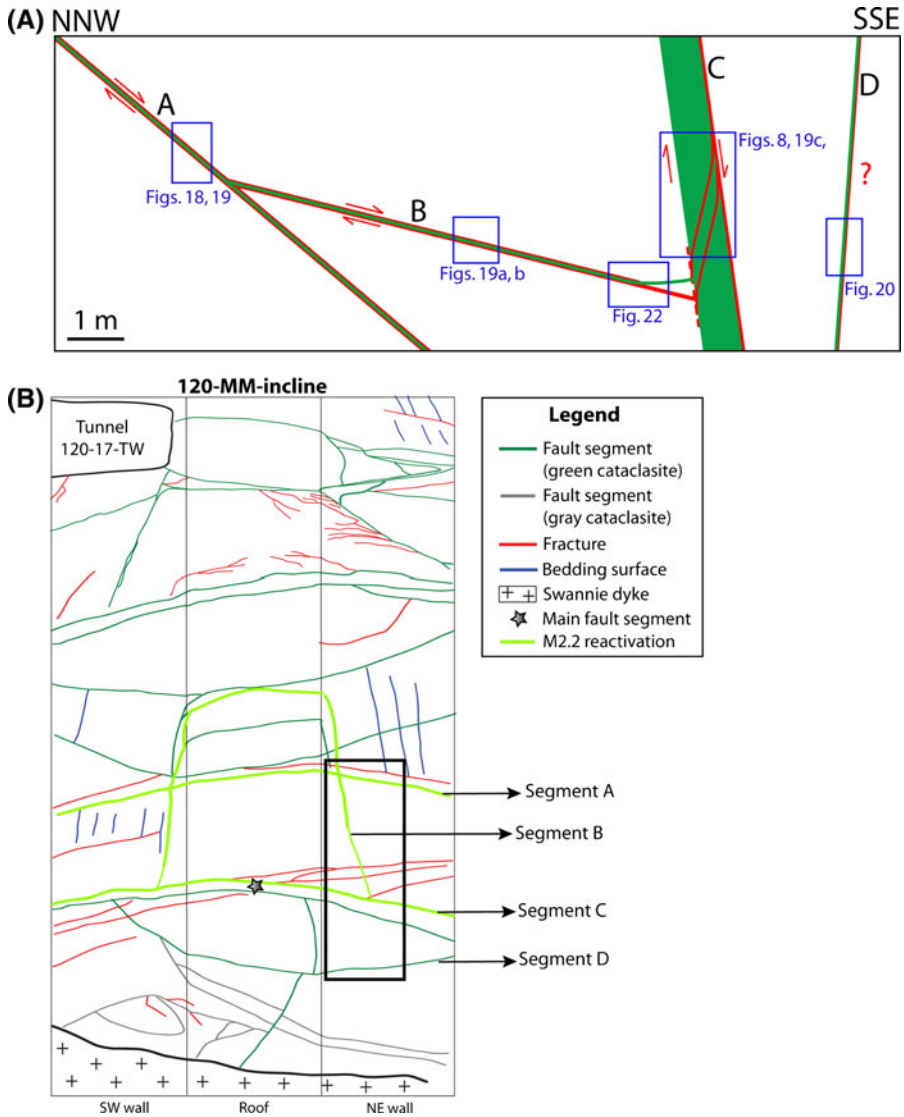

Figure 17

Structure of the 2004 M2.2 rupture-zone. **a** Schematic cross section of the rupture-zone with four reactived segments in the Pretorius fault-zone (marked *A–D*). *Green* cataclasite zones; *red* fresh rock-flour of the M2.2. **b** Tunnel map though the 120-MM-incline with marked reactivated segments and the location of the cross section in *A*

6. The thickness of fresh gouge zones range from 1 to 5 mm at a given position.

6. Discussion

6.1. Structural Development of the Pretorius Fault

Our interpretation of the development of the Pretorius fault is based on our mapping of faults and fractures in the tunnels and borehole images and on fault maps of the reef surfaces mapped by TauTona mine geologists (Table 1; Fig. 23). We envision the following process:

1. The faults mapped on the reef, set R (Table 1), are sub-parallel to the Pretorius fault, they locally displace the reef up to 3 m, and they form a ~100 m wide zone south of the fault (Fig. 23b). These faults are part of the Pretorius fault system and represent a relatively wide zone of gentle brittle deformation that developed during the early

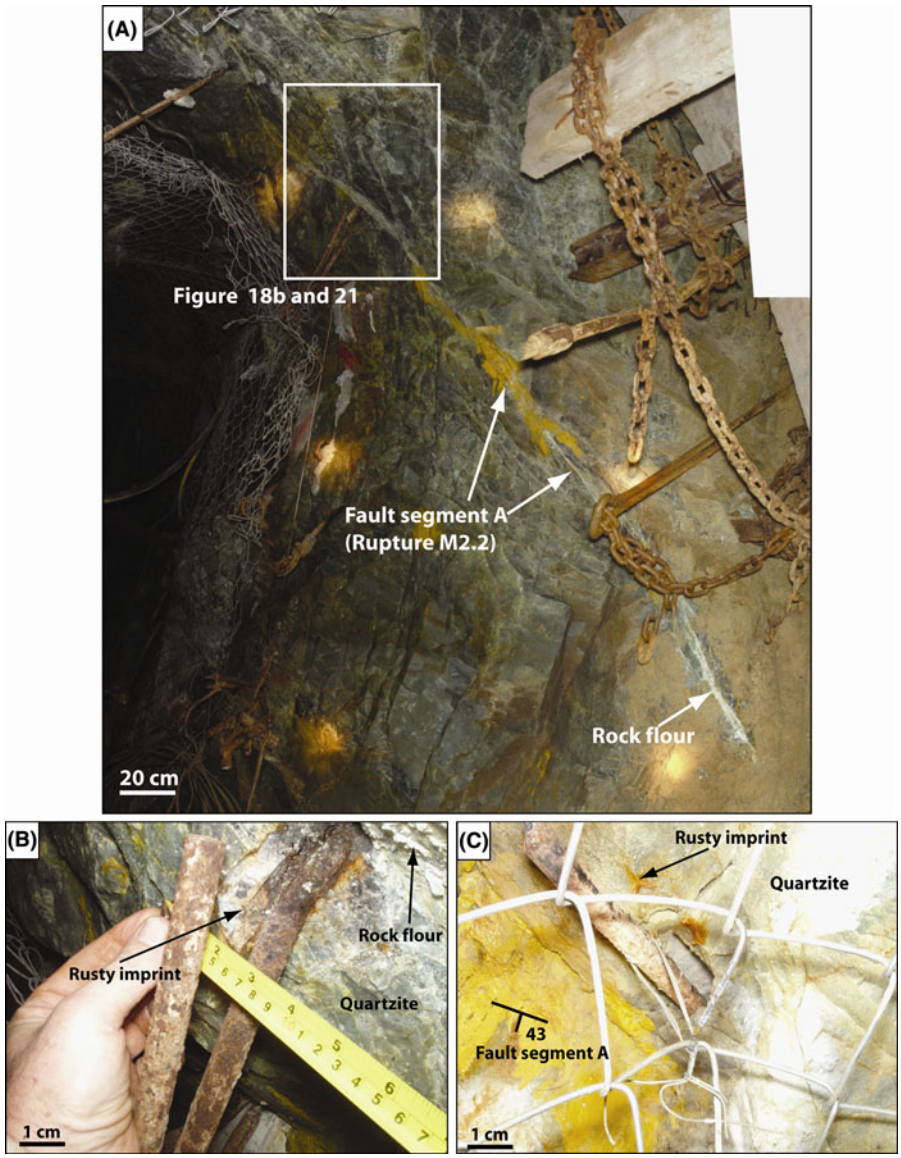

Figure 18
Rupture features of the M2.2 event, south side of 120-17-b tunnel. **a** Segment A, recognized by zones of fresh white rock-flour and displaced rock bolt with 25 mm displacement shown in (**b**); note the rusty imprint of the original position of the rock bolt. **c** Displaced rock bolt across segment A in the roof with displacement of 10 mm; note rusty imprint of the original position of the rock bolt

stages of the Pretorius fault growth before slip localization.

2. Fractures of sets T1, T2 and A (Table 1) strike generally parallel to the Pretorius fault, and they are found only within in the Pretorius fault-zone (Fig. 11). Many of these fractures carry cataclasite zones (Figs. 12, 17, 18) or slickenside striations. An important member of set A is the 'principal slip zone' (PSZ) described above (Fig. 8). We interpret that the high density these sets indicates the inward increase of damage of the Pretorius fault. The PSZ is the site of the localized slip of the fault (above).
3. Set B, which includes fractures sub-parallel to the bedding surfaces, is a special case. On one hand, they are found almost exclusively in boreholes outside the Pretorius fault-zone (boreholes 2, 3, 10, 7 V and 7S, in Fig. 11), and this distribution

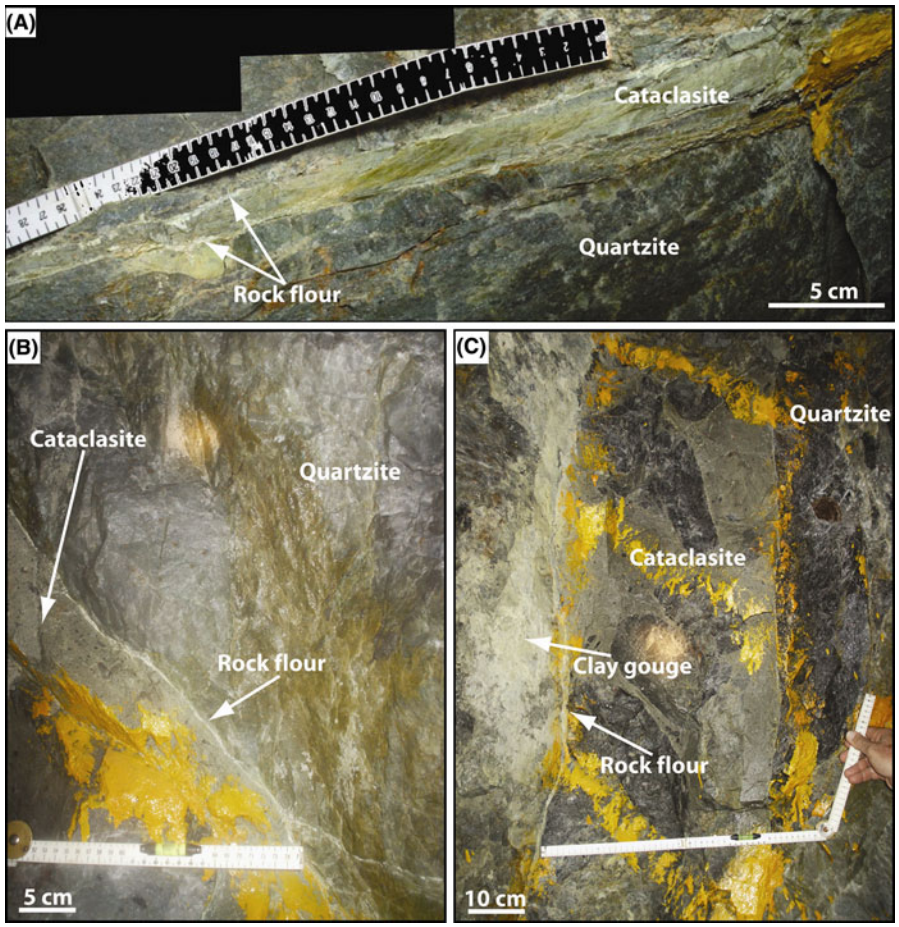

Figure 19
Cataclasite-quartzite contacts with rock-flour zones along reactivated segments of M2.2 rupture. **a** Close-up of the bedding-parallel segment B, 120-17-b tunnel; note rock-flour on both upper and lower contacts of the cataclasite. **b** Segment B in the NE-wall of the 120-MM-incline. **c** Rock-flour and clay gouge along the south contact segment C, which is PSZ (Fig. 8), in the SW-wall of the 120-MM-incline. Note rounded quartzite blocks within the fault segment of several tens of cm in diameter

suggests that they are not related to the Pretorius fault. However, in several locations, cataclasite zones are found along bedding surfaces (Fig. 17, 118-TW-Raise-120 tunnel), and one segment of the M2.2 rupture is a bedding surface (Fig. 18). We thus regard set B as pre-existing, weak sedimentary surfaces that are part of the Pretorius fault-zone.

4. Set C (sub-horizontal fractures) is enigmatic. It is found in only two boreholes (Daf5 and hole 13 in Fig. 11), it is not observed in the tunnels, and its orientation has no clear relations to the Pretorius fault. We suspect that these are tensile fractures that were induced by relaxation of vertical, gravitational load that is due to mining in the reef. In this respect, they are analogous to sheet fractures in granite bodies that form sub-parallel to the ground surface due to stress relaxation (JOHNSON, 1970).

We now discuss the development stage of the Pretorius fault. Fault zones are always associated with a damage zone (MITCHELL and FAULKNER, 2009), and the width of this damage zone can be correlated to the fault throw (SHIPTON and COWIE, 2001) or the fault length (KATZ *et al.*, 2003). In early stage of faulting, a significant amount of shear can be accommodated within the damage zone without slip

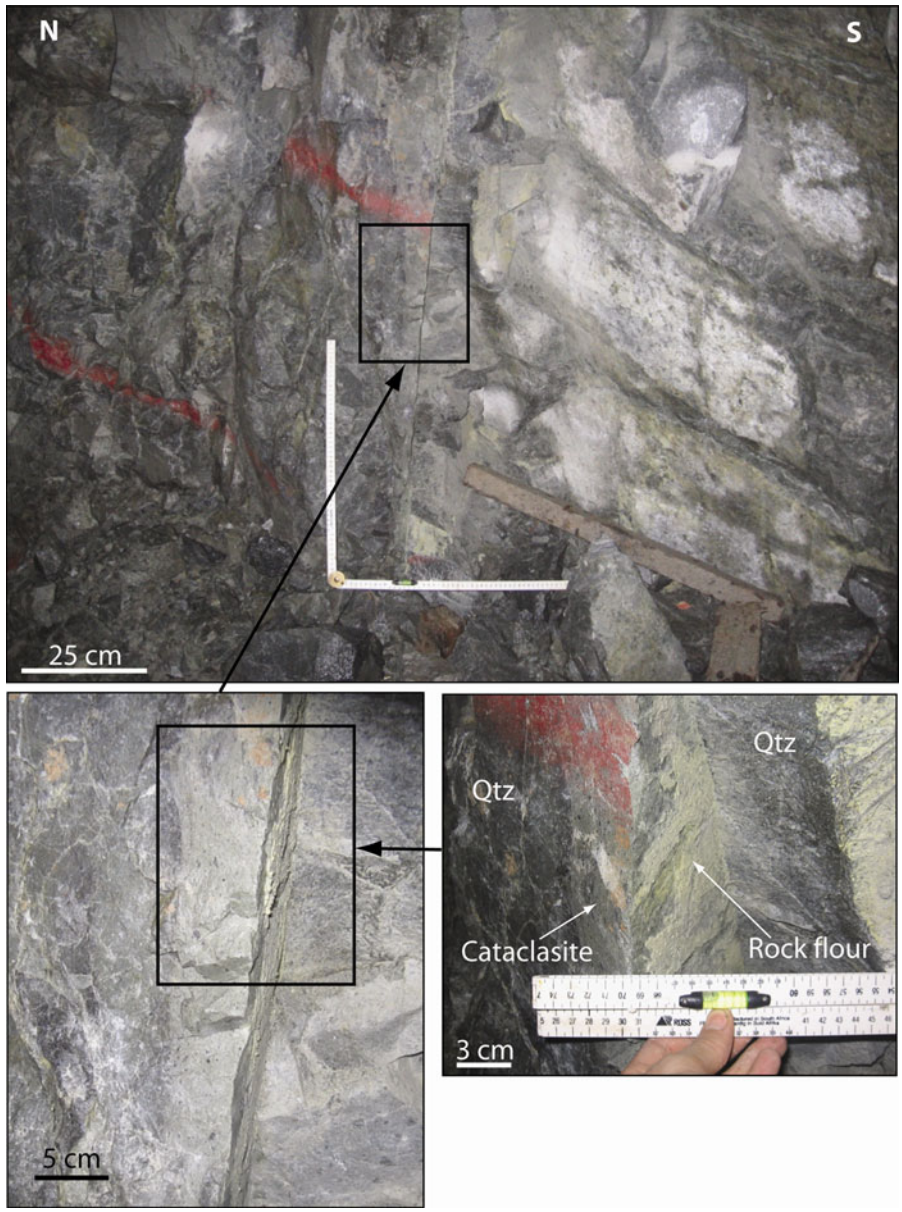

Figure 20
Segment D in the NE-wall of the 120-MM-incline. The south contact of this segment displays 1–2 mm thick zone of fresh rock-flour

localization (AYDIN and JOHNSON, 1978; KATZ *et al*., 2003). In a large, mature fault, the slip is highly localized as described by CHESTER *et al*. (1993) for the North San Gabriel fault, which is a segment of San Andreas system. They showed that this fault of about 44 km of slip has a ~200 m wide damage zone, a ~1 m thick cataclastic core with an inner ultracataclasite zone of ~1 cm thick of extreme slip localization. We envision that the Pretorius fault evolved similarly to the above path. Its network of multiple segments that carry small displacements is a relic of the early stage of its development equivalent to the damage zone mentioned above. The Pretorius fault entered the slip localization stage as manifested by the occurrence of the PSZ (Fig. 23c). The PSZ divides the fault-zone into a northern and southern blocks (above), it has a thick cataclasite zone (0.5–1 m), and it is continuous horizontally and

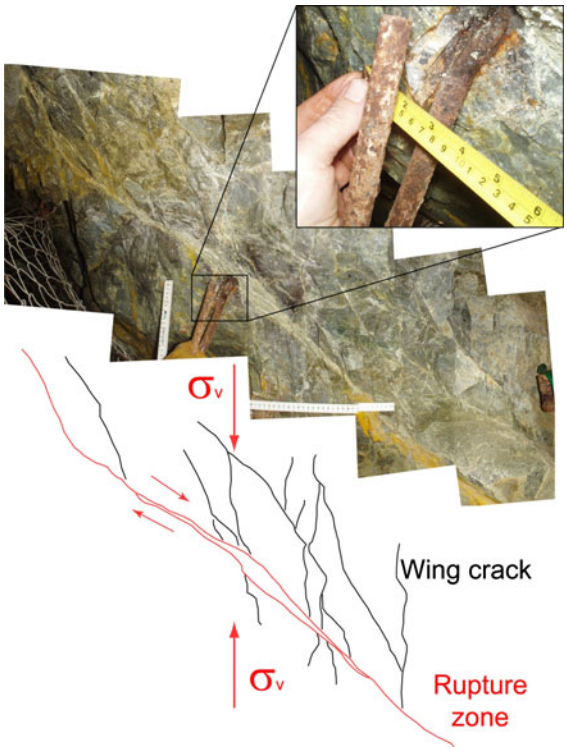

Figure 21
Secondary fractures associated with the M2.2 rupture in the hanging wall of segment A in 120-17-b tunnel. Upward concave structure of the fractures indicates mode I-II propagation away from the main rupture in the vertical direction (toward σ_v). *Inset* Location of the displaced rock bolt (Fig. 18)

vertically (above). The recent reactivation of the PSZ (Fig. 18) further supports the interpretation that the Pretorius fault entered the localized slip stage of a mature fault. A schematic cross section highlighting the main features of the Pretorius fault is presented in Fig. 24.

6.2. Origin of the Fault Rocks

Thin (~1 mm) and wide (~0.5 m) cataclasite zones appear along many fault segments in Pretorius fault-zone (above and Figs. 5, 6, 12). The cataclasite displays (1) a wide range of grain size distributions with coarse, angular to rounded fragments in an ultrafine grain matrix (Fig. 14); (2) intense thickness variations (Fig. 12); (3) flow structures on macro- and micro-scales (Figs. 12, 13, 14); (4) local occurrence of fabric in the ultra fine matrix (Fig. 14); (5) lack of shear fabric in the coarse clasts; (6) rare (local) evidence of melting; (7) composition similar to the host rocks; and (8) coloring in the gray–green–yellow range.

Similar cataclasites have been observed in South African faults. Killick *et al.* (1988) studied a large, bedding-parallel fault-zone in mines and boreholes in the West Rand area, about 40 km east of TauTona mine. They found fault rocks that are very similar, if not identical, to the cataclasites in TauTona mine and referred to these rocks as pseudotachylytes. Yet, they did not provide direct evidence for melt and commented that pseudotachylytes could form either by melting (e.g., Sibson, 1975) or by cataclasis (Wenk, 1978). In general, the term pseudotachylyte is reserved to rocks that formed by rock melting (Sibson, 1975; Reimold, 1995; Spray, 1995), and may occur as glass or in a devitrified form with evidence for melting (Lofgren, 1971) (e.g., 'snow flakes'). With only one local evidence for melt in our study (Zechmeister *et al.*, 2005), we refer to the ultrafine grain, cohesive, dark fault rock of Pretorius fault as cataclasite.

We propose that the observed cataclasites formed during Archaean seismic activity as a non-cohesive fine-grain gouge powder that could flow to form the abundant flow features on both macro- and micro-scales (above). Subsequently, this granular material was cemented, possibly by sintering at elevated temperature (above and Fig. 16). The sintering process likely occurred during the later stage of the Platberg rifting, as the Witwatersrand Basin underwent low-grade burial metamorphism up to lower greenschist grades, with peak metamorphism during the emplacement of the mafic and ultramafic Bushveld intrusion at 2,050 Ma that resulted in major thermal perturbation of the basin (Robb *et al.*, 1997). The 2.0 Ga period of tectonic inactivity contributed to continual strengthening of the cataclasite to its current massive, cohesive state.

6.3. Earthquake Rupture Zone

The NELSAM site provides a rare opportunity to analyze the rupture zone of a single earthquake along a large fault at focal depth. The M2.2 event reactivated the Pretorius fault, an Archaean fault that has been inactive for at least 2 Ga and was subjected to cementation and sintering of the ancient gouge zones.

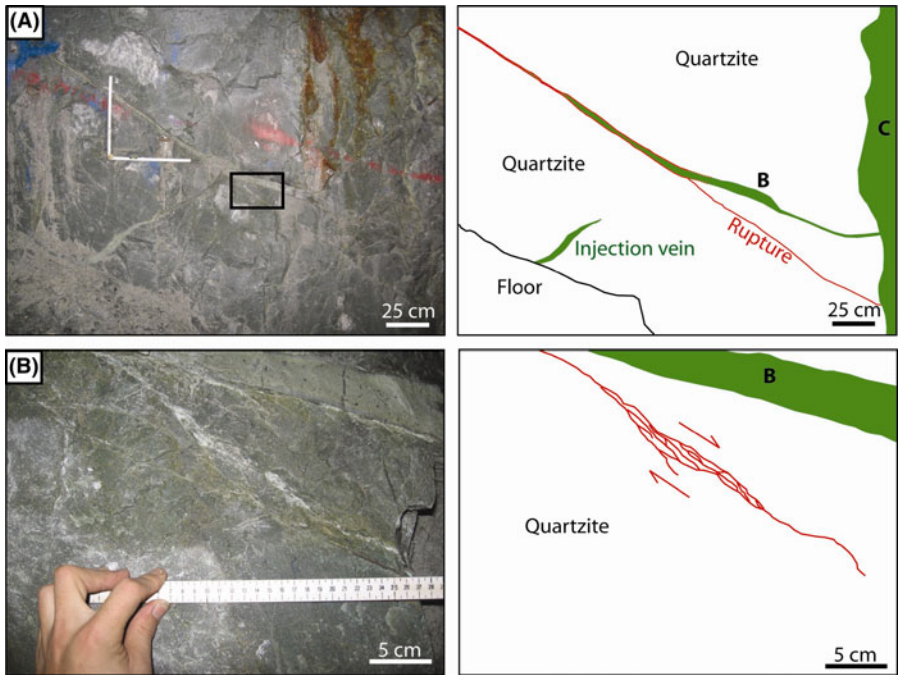

Figure 22
Rupture zone along segment B in 120-MM-incline near the intersection with segment C. **a** *Left* general view; *right* lithology and traced fractures; note that the segment deflects to horizontally and branches with one branch following the cataclasite-quartzite contact, and the other cuts across intact rock. **b** Close up of A, showing widening of the rupture-zone to form a 1–2 cm wide zone of multiple Riedel fractures that are compatible with normal slip

Table 1

Fracture sets associated with the Pretorius fault-zone

Mapping sites	Set notation	Mean attitude	Structural interpretation	Comments	Figure
Tunnels (levels 118 and 120)	T1	69°/170° ± 17°	Fault surfaces within Pretorius fault-zone	May contain cataclasite	8
	T2	72°/346° ± 9°			
Borehole image analyses	A	66°/139° ± 12°	Fault surfaces within Pretorius fault-zone	Found only in borehole Daf5	11, 12b
	B	30°/169° ± 14°	Bedding and fault surfaces	Found in most boreholes	11, 12
	C	06°/120° ± 12°	Mining related fractures	Relief of vertical load	11, 12
Reef mapping	R	050° ± 14°	Faults related to the Pretorius fault	Faults, dip to north and south	20, 21

These processes had strengthened and lithified the Pretorius fault-zone and its fault rocks, and we thus expected that the fault weakness zonation which developed during the Archaean activity would disappear. The observed rupture-zone of the 2004 M2.2 earthquake did not follow these predictions:

1. *Observed* The earthquake slip occurred primarily along pre-existing segments (Figs. 8, 17, 18, 19, 20).

   Expected Many new fractures across intact rock (e.g., Gay and Ortlepp, 1979).

2. *Observed* The slipping segments are fairly planar (Figs. 17, 18).

   Expected Networks of multiple branching fractures; such networks appear only locally (Figs. 21, 22).

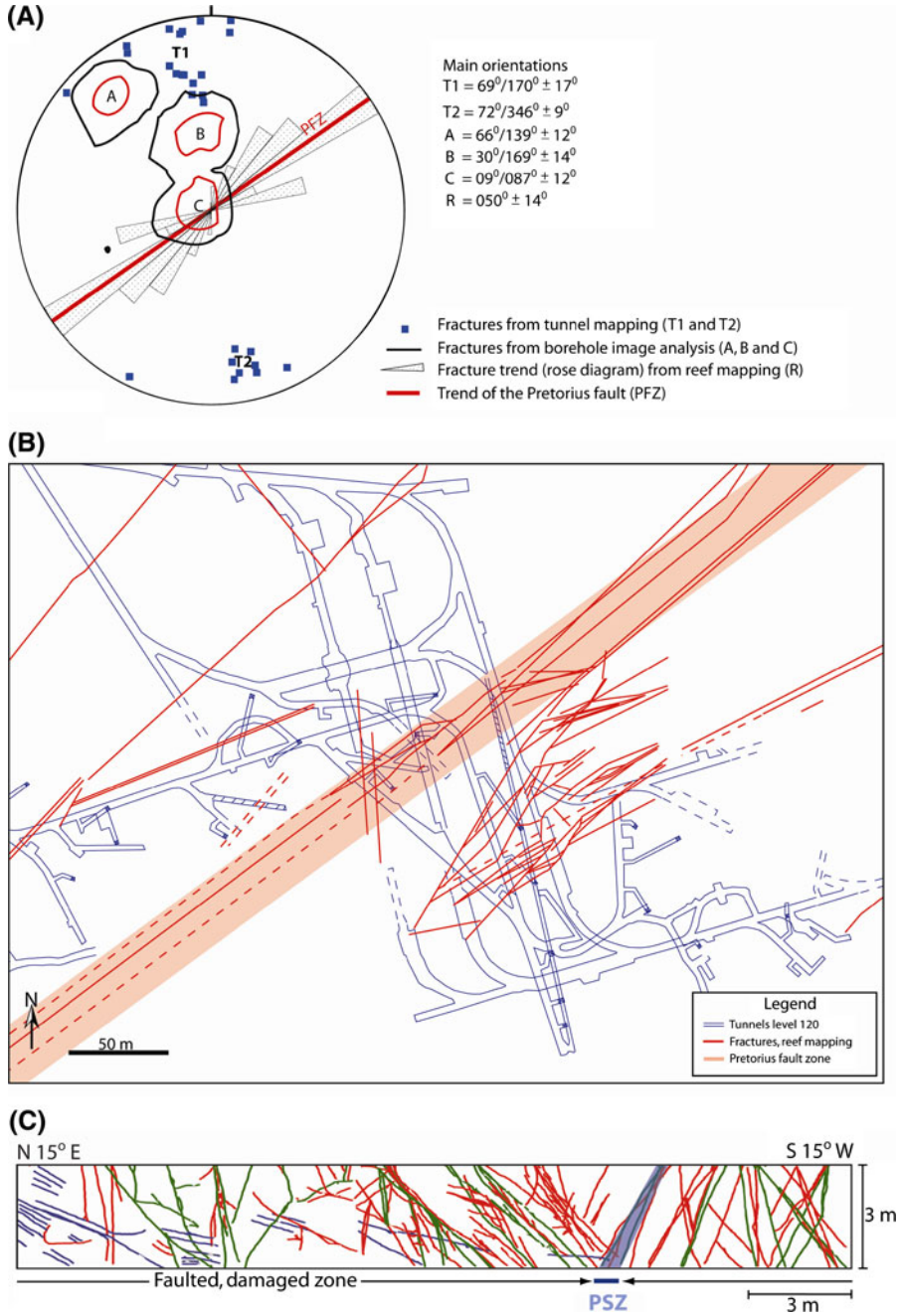

Figure 23

The structure of the Pretorius fault-zone. **a** Synthesis of orientation data of faults and fracture of the Pretorius fault-zone in NELSAM site. The data include fracture sets T1 and T2 from 118-xcut tunnel (location in Fig. 5), set *A*, *B* and *C* from borehole image analysis (Fig. 10), fractures from reef mapping, and the general trend of the Pretorius fault. See text for interpretations. **b** Fault and fracture map of the mined reefs in the NELSAM site kindly provided by the geology team of TauTona mine. The fault traces are projected on top of the tunnel network of level 120 (*blue*). **c** A generalized cross-section of the Pretorius fault-zone that is based on the tunnel map in 118-xcut tunnel (Fig. 5). Note the multiple branching segments, the thick principal slip zone (*PSZ*) that separates the bedding-surface rich northern block from the southern block (details in *text*)

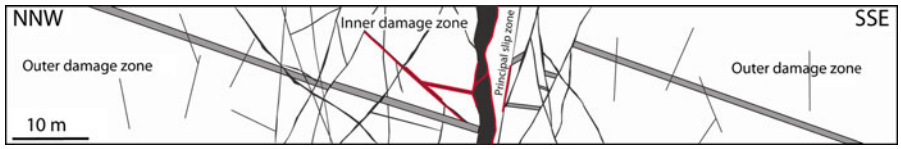

Figure 24
Schematic cross section of the main features that characterize the Pretorius fault zone. *Highlighted* is the outer and inner damage zone, as well as the principle slip zone

3. *Observed* The slipping segments are not parallel to each other (Fig. 17).

   Expected Sub-parallel segments that are oriented in favorable direction to the in situ stresses (analysis in Part II).

4. *Observed* Slip is associated with the formation of fine-grain gouge (rock-flour) layers with thicknesses of 1–5 mm (Figs. 18, 19, 20).

   Expected As observed: Rock-flour is common to shear failure of quartzite in South African mines (Dor *et al*., 2001; Gay and Ortlepp, 1979; Olgaard and Brace, 1983; Ortlepp, 2000; Stewart *et al*., 2001) and in our lab experiments (Part II).

5. *Observed* Slip is localized along the contacts between the cataclasite of the ancient fault segment and the quartzitic host rock (Figs. 18, 19, 20).

   Expected Similar localization was observed in rock-mechanics experiments (Part II), and other works, (e.g., Engelder, 1974).

7. Conclusions

The Pretorius fault, TauTona mine, South Africa, is a $\sim$10 km long, oblique-strike-slip fault with oblique displacement of up to 200 m. In our analysis we identified three structural zones within the Pretorius fault-zone: (1) an outer damage zone, $\sim$100 m wide, of brittle deformation manifested by multiple widely spaced fractures and faults with slip up to 3 m. (2) an inner damage zone, 25–30 m wide, with high density of anastomosing conjugate sets of fault segments and fractures, many of which carry cataclasite zones (Fig. 23). (3) a single, dominant segment, with a cataclasite zone up to 0.5 thick, is the PSZ that accommodated most of the slip of the Pretorius fault (Figs. 8, 17, 23). This fault-zone structure indicates that during its Archaean activity, the Pretorius fault entered the stage of slip localization with multiple events along a single PSZ (Fig. 8).

The Pretorius fault slip during Archaean times was associated with comminution of large volumes of the quartzitic rocks and the formation of thick gouge zones. The gouge was mobilized and formed injection veins that penetrated the host rocks and bedding surfaces. During the long period of inactivity and under elevated temperature, this incohesive gouge was cemented and sintered into the green to gray cataclasite zone found today.

We mapped the rupture-zone of the 2004 M2.2 earthquake that reactivated the Pretorius fault at 3.6 km depth. The M2.2 rupture-zone reveals that (1) slip occurred almost exclusively along four pre-existing, large, quasi-planer segments of the ancient fault-zone; (2) the slipping segments include the ancient PSZ; (3) the reactivated segments are not parallel to each other; (4) gouge zones, 1–5 mm thick, composed of white rock-flour formed almost exclusively along the cataclasite-host rock contacts of the slipping segments; (5) locally, new fractures branched from the slipping segments and propagated in mixed shear-tensile mode; (6) the maximum observed shear displacement is 25 mm in oblique-normal slip. The mechanical analysis of the rupture-zone is presented in Part II.

Acknowledgments

We are in debt to many people and organizations. Foremost to Gerrie van Aswegen of ISS International who guided and advised us throughout this entire

study. This work was not possible without the invaluable help and support by Hannes Moller, Pieter van Zyl, Rob Burnet, and many other workers in TauTona mine and ISSI. We greatly appreciate the help in underground work by Tom Dewers, Amir Allam, Kate Moore, and Matthew Zechmeister of University of Oklahoma, Reginald Domoney, Selwyn Adams, and Curnell Campher, of the University of Western Cape, South Africa, Amie Lacier of Stanford University, and Malcolm Johnston, US Geological Survey. This work could not be completed without the important advice, suggestions and encouragement by the NELSAM team of Tom Jordan, Malcolm Johnston, Mark Zoback, TC Onstott, and well as Hiroshi Ogasawara, Ritsumeikan University, Japan, and Uli Harms, GFZ, Germany. Many thanks to AngloGoldAshanti for the permission to work in the TauTona mine and the generous logistic support. The thoughtful comments of two anonymous reviewers significantly improved the manuscript. This work was supported by the National Science Foundation under Grant No. 0409605 (NELSAM project), and the drilling grant by ICDP (DAFSAM project). Other sponsors of this work include US Geological survey, AngloGoldAshanti, ISS International, and National Research Foundation (NRF).

References

Anderson, A.T. Jr. (1991), *Hourglass inclusions: Theory and application to the Bishop Rhyolitic Tuff*. American Mineralogist, *76*, 530-547.

Armstrong, R.A., Compston, W., Retief, E.A., Williams, I.S., and Welke, H.J. (1991), *Zircon ion microprobe studies bearing on the age and evolution of the Witwatersrand triad*, Precambrian Research, *53*, 243-266.

Aydin, A., and Johnson, A.M. (1978), *Development of faults as zones of deformation bands and as slip surfaces in sandstone*: Pure and Applied Geophysics, *116*, 931-942.

Boettcher, M.S., McGarr, A., and Johnston, M. (2009), *Extension of Gutenberg-Richter distribution to Mw -1.3, no lower limit in sight*, Geophys. Res. Lett., *36*, L10307. doi:10.1029/2009GL038080.

Boettcher, M.S., McGarr, A., Johnston, M., van Aswegen, G., Heesakkers, V., and Reches, Z. (2006), *Analysis of a M2.2 Earthquake in TauTona Gold Mine, South Africa, and Estimate of its Energy Budget*, Eos Trans. AGU, *87*(52), Fall Meet. Suppl., Abstract S43C-06.

Brady, B.H.G., and Brown, E.T., Rock mechanics for underground mining (2nd. ed. Chapman and Hall, London 1993).

Chester, F.M., Evans, J.P., and Biegel, R.L. (1993), *Internal structure and weakening mechanisms of the San Andreas Fault*, J. Geophys. Res. *98*, 771-786.

Cook, N.G.W., (1963), The seismic location of rockbursts, In Proc. Rock Mechanics Symposium, 5th, Pergamon Press, Oxford, p. 493.

Dor, O., Reches, Z., and van Aswegen, G. (2001), Fault zones associated with the Matjhabeng earthquake 1999, South Africa: Rockbursts and Seismicity in Mines, RaSiM5 (Proceedings), South African Inst. of Mining and Metallurgy, 109–112.

Engelder, J.T. (1974), *Cataclasis and the Generation of Fault Gouge*, Geol. Soc. Am. Bull., *85*, 1515-1522.

Frimmel, H.E., and Minter, W.E.L. (2002), Recent developments concerning the geological history and genesis of the Witwatersrand gold deposits, South Africa, Society of Economic Geologists Special Publication, 9, 17-45.

Gay, N.C., and Ortlepp W.D., (1979), *Anatomy of a mining-induced fault zone*, Geological Society of America Bulletin, *90*, 47-58.

Germanovich, L.N., Salganik, R.L., Dyskin, A.V., and Lee, K.K. (1994), *Mechanisms of brittle fracture of rock with pre-existing cracks in compression*, Pure App. Geophy., *143*, 117-149.

Gibowicz, S.J., and Kijko, A. (1994), An Introduction to Mining Seismology, Academic Press, San Diego.

Gibson, M.A.S., Jolley, S.J., Barnicoat, A.C., and Gochioco, L.M. (2000a), *Interpretation of the Western Ultra Deep Levels 3-D seismic survey*, The Leading Edge, *19*, 730-735.

Gibson, R.L., Reimold, W.U., Phillips, D., and Layer, P.W. (2000b), (*super 40*) *Ar*/(*super 39*) *Ar constraints on the age of metamorphism in the Witwatersrand Supergroup, Vredefort Dome* (*South Africa*), South African Journal of Geology, *103*, 175-190.

Grice, A.G. (1998), Underground mining with backfill, Proceedings of the 2nd Annual Summit -Mine Tailings Disposal Systems, Brisbane, Australia, 234–239.

Heesakkers, V., Murphy, S., and Reches, Z, 2011 (Part II). Earthquake Rupture at Focal Depth, Part II: Mechanics of the 2004 M2.2 Earthquake Along the Pretorius Fault, TauTona mine, South Africa (this volume).

Holdsworth, R.E., Butler, C.A. and Roberts, A.M. (1997), *The recognition of reactivation during continental deformation*, Journal of the Geological Society, *154*, 73-78.

Huntoon, P.W, Synopsis of Laramide and post-Laramide structural geology of the eastern Grand Canyon, Arizona, In Geology of Northern Arizona, Part 1 (ed. Eastwood, R.L., Karlstrom, T.N.V., Swann, G.A.) (Flagstaff, Arizona 1974) pp. 317-355.

Johnson, A.M., Physical Processes in Geology (ed. Freeman, W.H.) (New York 1970).

Kamo, S.L., Reimold, W.U., Krogh, T.E., and Colliston, W.P. (1996), *A 2.023 Ga age for the Vredefort impact event and a first report of shock metamorphosed zircons in pseudotachylitic breccias and granophyre*, Earth and Planetary Science Letters, *144*, 369-387.

Katz, O., Reches, Z., and Baer, G. (2003), *Faults and their associated host rock deformation: Part I. Structure of small faults in quartz-syenite body, southern Israel*, Journal of Structural Geology, *25*, 1675-1689.

Killick, A., Thwaites, A., Germs, G., and Schoch, A. (1988), *Pseudotachylite associated with a bedding-parallel fault zone between the Witwatersrand and Ventersdorp Supergroups, South Africa*, Geologische Rundschau, *77*, 329-344.

Lin, A. (1994), *Microlite Morphology and Chemistry in Pseudotachylite, from the Fuyun Fault Zone, China*, The Journal of Geology, *102*, 317-329.

LIPPMANN-PIPKE, J., ERZINGER, J., ZIMMER, M., KUJAWA, C., BOETTCHER, M.S., MOLLER, H., VAN HEERDEN, E., BESTER, A., RECHES, Z., (2009), *Long-term, on-site borehole monitoring of gases released from an "active" fault system at 3.6 km depth, TauTona Gold Mine, South Africa*, AGU, Fall Meet. Suppl., Abstract H21 J-04.

LOFGREN, G. (1971), *Experimentally Produced Devitrification Textures in Natural Rhyolitic Glass*, Geological Society of America Bulletin, *82*, 111-124.

LUCIER, A.M., ZOBACK, M.D., HEESAKKERS, V., RECHES, Z., AND MURPHY, S.K. (2009), *Constraining the far-field in situ stress state near a deep South African gold mine*, International Journal of Rock Mechanics and Mining Sciences, *46*, 555-567.

MARONE, C. (1998), *The effect of loading rate on static friction and the rate of fault healing during the earthquake cycle*, Nature, *391*, 69-72.

MCCARTHY, T.S., STANISTREET, I.G., and ROBB, L.J. (1990), *Geological studies related to the origin of the Witwatersrand Basin and its mineralization; an introduction and a strategy for research and exploration*, South African Journal of Geology, *93*, 1-4.

MCGARR, A., (1984), Some applications of seismic source mechanism studies to assessing underground hazard: Rockburst and Seismicity in Mines, In Symp. Ser. No. 6, South African. Inst. Min. Metal., (ed Gay, N.C. and Wainwright, E.H.), Johannesburg, 199-208.

MENDECKI, A.J., Seismic Monitoring in Mines, (ed. Mendecki, A.J.) (Chapman and Hall, London 1997).

MITCHELL, T.M. and FAULKNER, D.R., (2009), *The nature and origin of off-fault damage surrounding strike-slip fault zones with a wide range of displacements: A field study from the Atacama fault system, northern Chile*. Journal of Structural Geology, *31*, 802-816.

MUHURI, S.K., DEWERS, T.A., SCOTT, T.E., and RECHES, Z. (2003), *Interseismic fault strengthening and earthquake-slip instability; friction or cohesion*?, Geology, *31*, 881-884.

OGASAWARA, H., S. SATO, S. NISHII, N. SUMITOMO, H. ISHII, Y. IIO, S. NAKAO, M. ANDO, M. TAKANO, N. NAGAI, T. OHKURA, H. KAWAKATA, T. SATOH, K. KUSUNOSE, A. CHO, M. MENDECKI, A. CICHOWICS, R. E. GREEN, and M. O. KATAKA., *Semi-controlled seismogenic experiments in South Africa deep gold mines*, J. South Afr. Int. Mining Metallurgy, *102*, 243–250, 2002a.

OGASAWARA, H., S. SATO, S. NISHII, H. KAWAKATA., and The Research Group of Semi-Controlled Earthquake-Generation Experiments in South African Deep Gold Mines, Temporal variation of seismic parameters associated with an Mw $\sim$ 2 event monitored at a 100 $\sim$ 200 m distance, in Seismogenic process monitoring, edited by Ogasawara, H., T. Yanagidani, and M. Ando, Balkema, Rotterdam, pp. 173–184, 2002b.

OLGAARD, D.L., and BRACE, W.F. (1983), *The microstructure of gouge from a mining-induced seismic shear zone*, Int. J. Rock Mechanics Mining Sci. Geomechanics Abs., *20*, 11-19.

ONSTOTT, T., CHAN, E., VAN HEERDEN, E., LITTHAUER, D., BESTER, A., RECHES, Z., VAN ASWEGEN, G., MOLLER, H., LIPPMANN-PIPKE, J. (2008), An in situ bioseismicity experiment 3.6 km beneath the surface at NELSAM, AGU, Fall Meet. Abstract H53A-1009.

ORTLEPP, W.D. (1992), *Note on fault-slip motion inferred from a study of micro-cataclastic particles from an underground shear rupture*, Pure and Applied Geophysics, *139*, 677-695.

ORTLEPP, W.D. (2000), *Observation of mining-induced faults in an intact rock mass at depth*, International Journal of Rock Mechanics and Mining Sciences, *37*, 423-436.

RECHES, Z., (1978), Development of monoclines: Part I, structure of the Palisades Creek branch of the East Kaibab monocline, Grand Canyon, Arizona, In Laramide Folding Associated with Basement Block Faulting in the Western United States (ed. Matthews, V.), Geological Society of America, *151*, 235-273.

RECHES, Z. (1988), *Evolution of fault patterns in clay experiments*, Tectonophysics, *145*, 141-156.

RECHES, Z., (2006), *Building a natural earthquake laboratory at focal depth*, Scientific Drilling, *3*, 30-33.

RECHES, Z., and LOCKNER, D.A. (1994), *Nucleation and growth of faults in brittle rocks*, J. Geophys. Res., *99*, 18159-18173.

RECHES, Z., and ITO, H., Scientific drilling of active faults: past and future, In Scientific Drillings Continental Scientific Drilling A Decade of Progress, and Challenges for the Future (ed. Harms, U., Koeberl, C., and Zoback, M.D.) (Springer 2007), 235-258.

REIMOLD, W.U. (1995), *Pseudotachylite in impact structures – generation by friction melting and shock brecciation?: A review and discussion*, Earth-Science Reviews, *39*, 247-265.

ROBB, L.J., CHARLESWORTH, E.G., DRENNAN, G.R., GIBSON, R.L., and TONGU, E.L. (1997), *Tectono-metamorphic setting and paragenetic sequence of Au-U mineralisation in the Archaean Witwatersrand Basin, South Africa, Australian Journal of Earth Sciences*, *44*, 353-371.

SHIPTON Z.K., and COWIE P.A., (2001), *Damage zone and slip-surface evolution over μm to km scales in high-porosity Navajo sandstone*, Utah., J Structural Geology, *23*, 1825-1844.

SIBSON, R.H. (1975), *Generation of Pseudotachylyte by Ancient Seismic Faulting*, Geophysical Journal of the Royal Astronomical Society, *43*, 775-794.

SIBSON, R. H. (1985), *A note on fault reactivation*, Journal of Structural Geology, *7*, 751-754.

SPOTTISWOODE, S.M., and MCGARR, A. (1975), *Source parameters of tremors in a deep-level gold mine*, Bull. Seism. Soc. Am., *65*, 93-112.

SPRAY, J.G. (1995), *Pseudotachylyte controversy: Fact or friction*?, Geology, *23*, 1119-1122.

STEWART, R.A., REIMOLD, W.U., CHARLESWORTH, E.G., and ORTLEPP, W.D., (2001), *The nature of a deformation zone and fault rock related to a recent rockburst at Western Deep Levels Gold Mine, Witwatersrand Basin, South Africa*, Tectonophysics, *337*, 173-190.

SWANSON, S.E., and FENN, P.M. (1986), *Quartz crystallization in igneous rocks*, American Mineralogist, *71*, 331-342.

VAN ASWEGEN, G., and BUTLER, A.G., Applications of Quantitative Seismology in SA Gold Mines, In Rockbursts and Seismicity in Mines (ed. Young, R.P.) (Balkema, Rotterdam 1993).

WARD, J.A., SLATER, G.F., MOSER, D.P., LIN, L.H., LACRAMPE-COULOUME, G., BONIN, A.S., DAVIDSON, M., HALL, J.A., MISLOWACK, B., BELLAMY, R.E.S., ONSTOTT, T.C., and SHERWOOD LOLLAR, B. (2004), *Microbial hydrocarbon gases in the Witwatersrand Basin, South Africa: Implications for the deep biosphere*, Geochimica et Cosmochimica Acta, *68*, 3239-3250.

WENK, H. R. (1978), *Are pseudotachylites products of fracture or fusion*?, Geology, *6*, 507-511.

YABE, Y., PHILIPP, J., NAKATANI, M., MOREMA G., NAOI, M., KAWAKATA, H., IGARASHI, T., DRESEN, G., OGASAWARA, H., and JAGUARS, (2009), *Observation of numerous aftershocks of an Mw 1.9 earthquake with an AE network installed in a deep gold mine in South Africa*. Earth Planets Space, *61*, e49–e52.

ZECHMEISTER, M.S., HEESAKKERS, V., MOORE, K., CAMPHER, C., and RECHES, Z. (2005), *Sintered cataclasite of the Archaean Pretorius fault zone, TauTona mine*, South Africa, Eos Trans. AGU, *86*(52), Fall Meet. Suppl, Abstract S31B-05.

(Received July 21, 2010, revised May 21, 2011, accepted May 23, 2011, Published online July 1, 2011)